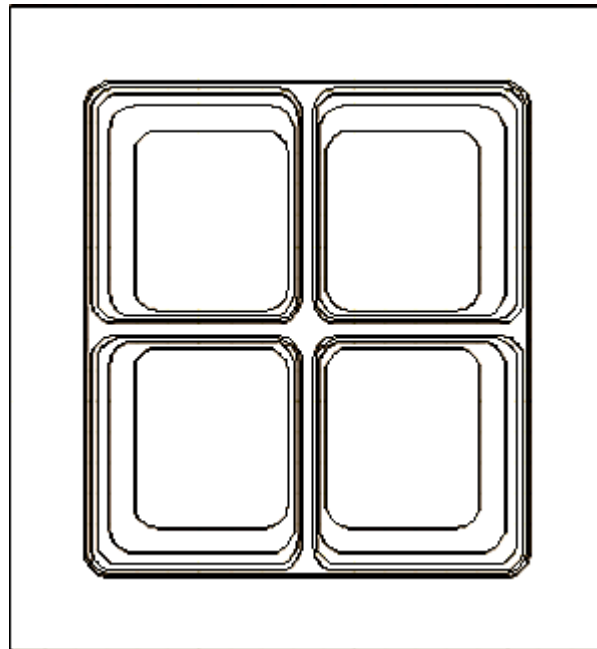


# Development of the Quad Focus GridPix Gaseous Tracking Detector



Kevin van 't Veer

Cover: top view, with the copper patterns, from a CAD drawing of the first Quad Focus drifter for the Quad Focus GridPix Gaseous Tracking Detector.

# Development of the Quad Focus GridPix Gaseous Tracking Detector

HBO Bachelor Graduation Report

By

Kevin van 't Veer

Hague University of Applied Sciences, Delft

drs. M.C. Vloemans

dr. ir. C. A. Swarts

National Institute for Subatomic Physics, Amsterdam

prof. dr. ir. H. van der Graaf



# Abstract

A Quad Focus GridPix Gaseous Tracking Detector is under construction, to allow calibration and test beam measurements to validate the working principles of the (quad) GridPix detectors while using a focused electric field. The development is well on its way: both measurements should be able to be conducted in the near future.

The detector is based on the GridPix sensor which is a Micromegas detector using the Medipix family of chips. The Medipix family of chips are charge sensitive pixel based CMOS chips. Specifically the TimePix1 chips are used. They allow for clocked measurements adding a third dimension to the measurements, i.e. time. The Micromegas detector is a modern version of the Geiger counter. A cathode foil is placed above a micro mesh structure which rests with insulating pillars on the readout anode. The cathode and the mesh have a high voltage potential applied creating an electric field. The electric field between the micro mesh and the readout anode is much greater than the field above the mesh. The whole is filled with a gas. An energetic charged particle is able to traverse this gas volume and ionize it, leaving behind a track of electron-ion pairs or clusters. The electrons will drift down to the readout anode due to the electric field. When passing through the micro mesh structure they will accelerate allowing them to release additional electrons which can in their turn release electrons. An electron avalanche is created, sufficient enough to be detected. Single electrons can be detected. The GridPix detectors are Micromegas detectors. The micro mesh structure is integrated on top of the Medipix chips. Each hole of the mesh (now a grid) has one aligned pixel. The insulating pillars do not cover the pixel input pads. This is achieved by wafer post processing.

Previously the GridPix gaseous detectors were tested using homogenous electric fields. The Quad Focus detector will use a focused electric field. This can reduce the production costs because a smaller readout surface is required to read the same or larger gas volumes. This requires calibration measurement to correct for the non-homogenous electric field and test beam measurement where there also is a magnetic field present which will alter the perceived tracks because the electric and magnetic field are not fully parallel to each other. Overall the feasibility of the corrections required when the detector is deployed (a magnetic field present) need to be assessed.

The gaseous tracking detector are promising to use as a tracking detector in for example the ATLAS project. Those detectors are able to record partial tracks from which the whole track can be reconstructed. Currently semiconductor based tracking detectors are used, which only result in a two dimensional measurement point from which the overall track has to be reconstructed.

One component of the GridPix detectors is the protection layer on top of the pixel input pads. Research and development of this layer resulted in a new method that allows for the measurement of high specific resistivity thin films which is based on the Micromegas detector.

# Contents

<b>1. The National institute for Subatomic Physics and Detector Research and Development .....</b>	<b>1</b>
1.1. Gaseous detectors and GridPix.....	1
1.2. The Quad Focus GridPix Gaseous Tracking Detector .....	2
<b>2. The Micromegas and GridPix Detectors.....</b>	<b>3</b>
2.1. The Micromegas detector .....	3
2.2. The Quad Focus Gaseous tracking detector .....	4
2.2.1. GridPix and Timepix1 .....	4
2.2.2. The Quad Focus Gaseous chamber.....	5
2.2.3. Effects of the electric field.....	6
2.2.4. Readout of the sensor .....	6
<b>3. Tracking .....</b>	<b>7</b>
3.1. Iron-55.....	7
3.2. Strontium-90.....	8
3.3. Alpha particles.....	10
3.4. Cosmic rays and test beams .....	11
<b>4. Functioning of the Quad Focus GridPix Gaseous Tracking Detector.....</b>	<b>12</b>
4.1. Preparation of the detector.....	12
4.2. Cosmic ray measurements .....	14
<b>5. The Quad Focus Drifter .....</b>	<b>16</b>
5.1. Initial design.....	16
5.2. Current design.....	16
5.3. Outlook.....	17
<b>6. Tracking with the Quad Focus detector, its calibration and future measurements.....</b>	<b>18</b>
6.1. Simulations of the focused electric field.....	18
6.2. Calibration of the Quad Focus drifter .....	19

<b>7. Measurement of the specific resistivity of potential protection layers for GridPix .....</b>	<b>20</b>
7.1. The Micromegas and measurement principles.....	20
7.2. The gas gain.....	21
7.2.1. Measureable quantities.....	21
7.3. Experimental setup .....	23
7.4. Results.....	24
7.5. Measurement remarks.....	27
<b>8. Conclusion.....</b>	<b>29</b>
<b>9. Future planning.....</b>	<b>30</b>
<b>Appendix.....</b>	<b>31</b>
A. A fit procedure for a Gompertz function .....	31
B. Resistive layer measurement results.....	33
DIMES sample 3.....	33
KAVLI 230 nm SiN .....	34
DIMES 662 nm SiN.....	35
C. Originele opdracht omschrijving.....	36
<b>References.....</b>	<b>37</b>
<b>Samenvatting.....</b>	<b>38</b>
<b>Dankwoord.....</b>	<b>39</b>

# 1. The National institute for Subatomic Physics and Detector Research and Development

The National Institute for Subatomic Physics (Nikhef) is a research institute of the Foundation for Fundamental Research on Matter. Its mission is “to study the interactions and structure of all elementary particles and fields at the smallest distance scale and the highest attainable energy”[1]. In its realization both accelerator-based particle physics and astroparticle physics are studied, on a theoretical and practical level. The practical side of those studies requires the detection of (elementary) particles in various (global) experiments. To achieve this, detectors are built with constant research and development carried out at Nikhef’s Detector Research and Development (R&D) department.

There are two main lines of research at Detector R&D. Both rely on the Medipix chips. The difference lies in the used mechanic that allow particles to be detected. One detection method is based on a semiconductor bonded to the Medipix chip and the other on building a gaseous chamber on top of the Medipix chip in which the Medipix chips are used as the readout anode. This report is about the development of the gaseous detectors.[2]

The Medipix family of chips is a CMOS pixel based imaging chip with initial and ongoing development for the needs of experiments conducted at the Large Hadron Collider (LHC) at CERN, Geneva (the European Organization for Nuclear Research) and other fields of science. During the second iteration of the Medipix chips, the Timepix chip was derived. This is a clocked version of the Medipix chip, adding an additional measurable dimension, i.e. time, to detectors utilizing this chip.[3]

## 1.1. Gaseous detectors and GridPix

There are many types of gaseous detectors. The first and most commonly known is the Geiger counter, able to count the number of ionizing events. From there on many evolved versions were invented. The multi-wire proportional chamber enabled the measurement of a track in a plane parallel to the detector. Different particles types could now be identified too. The addition of drift chambers, especially the Time Projection Chamber (TPC) was a major breakthrough and improved the resolution of gaseous detectors by applying an electric and magnetic field parallel to each other, reducing the diffusion of electrons originating from the ionizing particles. In origin the TPC was read by a wire chamber on the collecting end. Since then many new structures were developed to amplify the electrons and to detect them. Currently, the Micromegas (Micro Mesh Gaseous Structure) is one of the most promising detector. In a Micromegas a metal mesh is placed on top of insulating pillars. When an electric field is applied this structure will amplify incoming electrons (originated from ionizing particles traversing a gas chamber on top of this structure). The amplified signal can be read by a chip. In particular, Nikhef’s Detector R&D for gaseous detectors focusses on the GridPix, a type of Micromegas detector based on the Medipix family of chips. The fundamental difference between GridPix and a Micromegas is that each pixel has one

aligned hole in the grid, while the insulating pillars do not cover the pixels. This is achieved by wafer post processing of the Medipix chips. This report is about the development of a full GridPix detector based on the Timepix1 chip with a specially tailored gaseous detector in which the electric field is focused onto the chips.[4]

## **1.2. The Quad Focus GridPix Gaseous Tracking Detector**

The detector in development is based on the existing GridPix detectors. Its main goal is to reduce the production costs by focusing the electric field, reducing the surface that needs to be actively read. The focussed electric field will take care of the dead inter chip regions, part of which is also present on the actual chip. The focusing electric field will be a specific designed gaseous chamber (drifter). This drifter is subject to constant improvement. Because the lifespan of the Timepix chips are not guaranteed, the whole concept is executed in a way that the individual chips are relatively easily replaced. When a 2x2 matrix of Timepix chips shows good longevity the current best focusing drifter will be applied, after which its calibration, alignment parameters and height corrections, to ensure correct functionality, will be studied.

The goal of this study is to build a working GridPix detector consisting of four TimePix1 chips and to perform measurements during a test beam and with an existing calibration setup (a nitrogen laser). With the final goal in the overall study of the Quad Focus GridPix Gaseous tracking detector being track analysis of those measurements to prove and validate the principles behind the detector.

The Micromegas and the Quad Focus GridPix Gaseous Tracking Detector will be explained more in depth. The development will be reported as well as the results of any (intermediate) tests and other measurements conducted that are relevant to the development of the GridPix detectors.

## 2. The Micromegas and GridPix Detectors

The basic principles of the Micromegas will be explained and the adaptations made in relation to the GridPix sensors. All relevant concepts of the Quad Focus GridPix Gaseous Tracking Detector will be discussed.

### 2.1. The Micromegas detector

The Micro Mesh Gaseous Structure detector is a two dimensional proportional detector consisting of a gaseous chamber and a readout anode. Figure 1 shows a schematic drawing of the Micromegas detector.

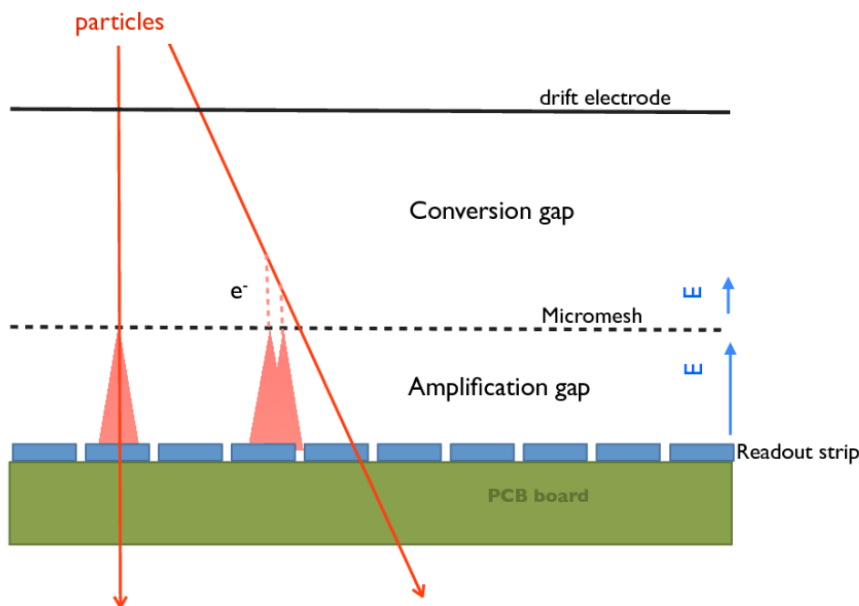


Figure 1. A Micromegas detector with the relative magnitude of the electric field and particles traversing the detector.

The gaseous chamber consists of the conversion gap and the amplification gap, which are separated by the micromesh structure, the grid. The grid is supported by insulating pillars that rest on the readout anode. The area in between the readout anode and the grid is the avalanche/amplification gap. Above the grid lies the conversion/drift gap which is sealed by a drift electrode, commonly referred to as the cathode. Perpendicular to this structure an electric field is created by supplying the cathode and grid with a separate high voltage potential. The readout anode is grounded. The field in the conversion and the avalanche gap are of different magnitude, defined by the potentials and the relatively large distance between the cathode and the grid and the small distance between the grid and the readout anode. The structure is filled with a gas. If a charged, high energetic particle traverses the gaseous chamber it can ionize the gas atoms or molecules, creating electron-ion pairs. Due to the electric field the ions drift to the cathode. The electrons will drift towards the anode. Passing the grid, the electrons are accelerated and able to ionize additional gas atoms or molecules releasing additional electrons which in their

turn can ionize the gas, resulting in an avalanche of electrons. An ionizing particle traversing the gaseous chamber is thus able to leave a track by creating electrons or clusters of electrons on its way. Those small signals are amplified, making them detectable.

The GridPix detectors function according to the same principles as the Micromegas detector.

## 2.2. The Quad Focus Gaseous tracking detector

The Quad Focus GridPix Gaseous Tracking Detector consist of various components, mainly dividable in the gaseous chamber and the GridPix sensor itself. The detector will be based on four, TimePix1 based, GridPix sensors in a 2x2 configuration. Each relevant component will be explained here.

### 2.2.1. GridPix and Timepix1

The GridPix sensor is a Micromegas in which chips from the Medipix family of chips are used as the readout anode, which is a pixel based charge sensitive CMOS chip. Every hole in the grid is aligned with one pixel. The insulating pillars which support the grid do not cover the actual pixels. Each chip contains 256x256 pixels, spaced 55  $\mu\text{m}$  from each other. Figure 2 shows a SEM picture with additional dimension sizes.

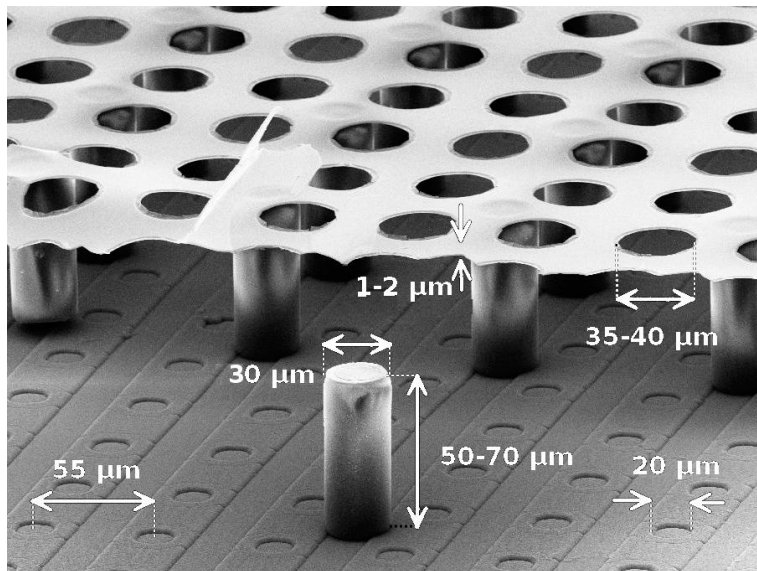
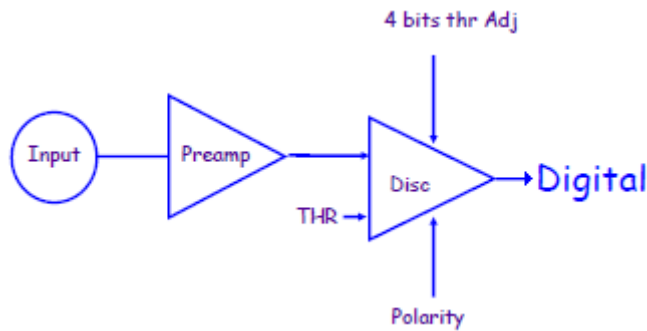


Figure 2. A SEM picture of a GridPix sensor with the dimensions of each component.[4]

Furthermore a dyke structure, made with an epoxy based negative photoresist (SU-8), is added at the edges of the GridPix covering some pixels, making them inactive. Those dykes act as a termination of the grid and reduces edge leakage currents, allowing for better shaping of the applied electric field at the edges.

The specific readout chip used in the development of the Quad Focus detector is the Timepix1 chip, based on the second iteration of the Medipix chips, able to measure both positive and negative charge. The threshold sensitivity requires a charge of 500 incident electrons. Each pixel has its separate analog and digital circuit. Figure 3 shows the analog part, consisting of a preamplifier, a discriminator with an on board 4 bits threshold adjustment and a programmable threshold level.



**Figure 3. The analog circuit of the pixels in the Timepix1 chip with THR the programmable threshold level.[4]**

The digital circuit contains a clock, a 100 MHz oscillator, allowing for measurement modes not available on the Medipix chips. The Timepix sensor is able to measure the amount of time that the threshold is exceeded – Time over Threshold (ToT) mode and measure the time between a hit and end of acquisition – Timepix mode (or Time of Arrival mode, ToA). Both Timepix and Medipix sensors are able to measure the amount of hits that exceed the threshold – Medipix mode.[4]

One component of the GridPix sensor is the protection layer on top of the readout chips. This layer protects the readout chip of large currents by limiting the flow of charge to the pixels. The layer is applied during wafer post processing. SiN (silicon nitride) layers are used of a few microns thick. To apply this layer, multiple deposition cycles are used to prevent the wafer from overheating. This method can introduce defects to the layer. Discharges are more likely to form in the defects. The protection layer and its development are important for GridPix in general and takes place continuously.

Parallel to the development of the Quad Focus GridPix detector, a new method for the measurement of high resistive layers is developed with great momentum and is reported in a further chapter (7).

### **2.2.2. The Quad Focus Gaseous chamber**

The gaseous chamber is the gas filled portion of the sensor. Its principles are already explained with the Micromegas detector. The gaseous chamber can be seen as introducing the conversion gap on top of the grid, which is present on the GridPix sensor. For the Quad Focus detector, the chamber will also contain a field cage. Copper wirings or strips are placed on the walls of the structure which are connected in series through resistors, from the cathode foil on top of the chamber. Each strip will thus have a small voltage drop, creating equipotential lines in the gaseous chamber allowing for a better shaped electric field. The electric field in the chamber can be shaped (focussed) by choosing the potentials. It also contains electrodes covering the dead inter chip regions of the 2x2 matrix. See figure 4 for an early concept of the drifter.

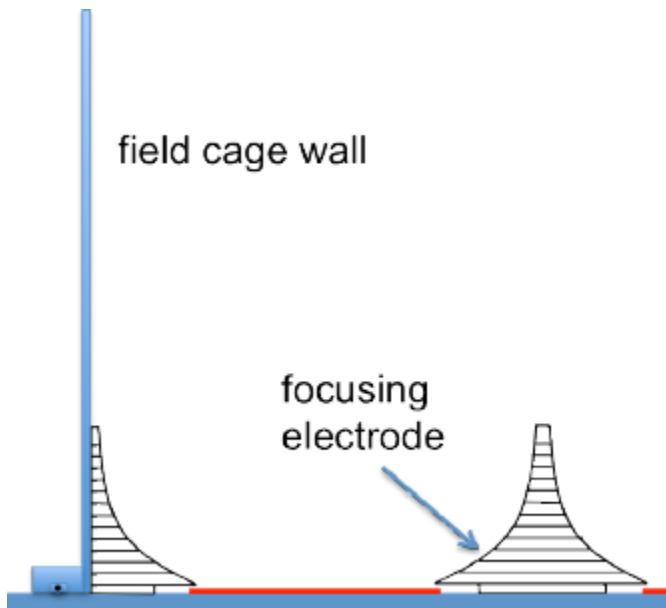


**Figure 4. Basic concept. Schematic side view of a single GridPix sensor (red) and the gaseous chamber depicted by the focusing electrodes and the field cage wall.**

Since the electric field is not fully perpendicular to the readout anode when the electric field is focused, a number of effects need to be taken in account.

### 2.2.3. Effects of the electric field

Focusing of the electric field in the GridPix gaseous detectors results in additional and new factors to take into account concerning the measurement data retrieved from the sensor when deployed. Electron-ion pairs created at  $x, y, z$  will result in a hit pixel  $x', y'$ . For a homogenous electric field  $x, y = x', y'$  and  $\Delta x, \Delta y = \Delta x', \Delta y'$ . For a focussed field  $x, y \neq x', y'$  and  $\Delta x, \Delta y \neq \Delta x', \Delta y'$ . This might alter the interpretation of the images retrieved from the sensors as possible diffusional effects (depending on the gas) from high originated electrons, might be different.

The deployed sensors are exposed to strong magnetic fields. Due to the magnetic field particles can be recognized by the curvature of their path such that the particle's momentum can be calculated which is used to identify it. Normally the electric and magnetic field would be parallel to each other. With the focused electric field however, the two fields cannot possibly be fully parallel to each other. Causing an alteration of the measurements due to the Lorentz force, since the electrons are moving with a velocity that makes a vector product with the magnetic field. This displacement needs to be corrected for.

### 2.2.4. Readout of the sensor

The readout portion of the sensor consist of standard electronics developed by Nikhef. The four Timepix1 GridPix sensor are placed on a ReNext QUAD board which contains the circuitry to connect each component of the GridPix sensor to the high voltage supplies. The same board connects to the RelaxD module which enables connection to a computer. The gas chamber is attached to the ReNext QUAD board. On the computer side the sensors are read with the Pixelman software, the standard software for Medipix made by the Medipix collaboration. Its main purpose is to retrieve the data and help through visualization of the retrieved data in early data acquisition stages. Actual processing of the data happens through other means (with ROOT, a data analysis framework by CERN) and is typically a study on its own. The RelaxD module allows for external triggering.

## 3. Tracking

Throughout this report various measurements that are conducted with the GridPix sensor for various purposes are mentioned. Those measurements are generally referred to as measuring events or tracks. The events and tracks are a result from the interactions of various particles with the gas in the gaseous drifter. The results depend on the used gas, the traversing particle and the detector in general. Various measurements that are mentioned will be explained including cosmic ray and test beam measurements.

The gaseous detectors are proportional detectors. The output is proportional to the original signal. The electron avalanches created can be described as a Townsend discharge[6]. The detector is able to measure single electrons. With high charge density ionising particles actual gas discharges can take place. The chips cannot withstand those high currents resulting in a breakdown of the chip. This is currently the limiting factor of the GridPix detectors. However the gas gain can be freely chosen through the strengths of the electric fields (generally in the order of 1 kV/cm in the conversion gap and 10kV/cm in the avalanche gap). Research is ongoing in improving the lifespan of the chips and/or making them discharge proof.

### 3.1. Iron-55

The iron-55 ( $^{55}\text{Fe}$ ) isotope decays into manganese. It has a complex interaction with gas with a net result a spectrum shown in figure 5. It is a well-defined spectrum that is suitable to access the functionality and precision of measurements related to the gaseous chamber and its electric field.

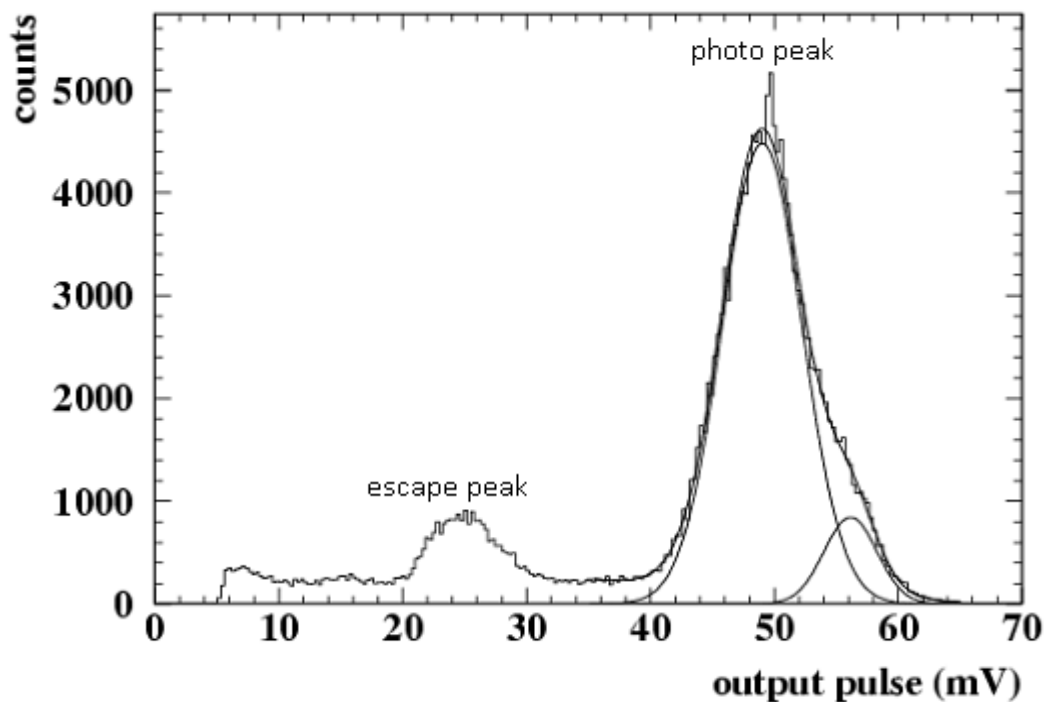


Figure 5.  $^{55}\text{Fe}$  spectrum showing the measured amplitude and the amount of occurrences. Measured with a GridPix detector. Specific conditions; gas: Ar/ $i\text{C}_4\text{H}_{10}$  80/20, Grid voltage: -400 V, drift field 1 kV/cm. The photo peak is due to the conversion of 5.9 keV and 6.4 keV X-ray quanta. [6]

The events that are measured are typically clusters of various sizes, with a distributed arrival time.



Figure 6. Two  $^{55}\text{Fe}$  ionization events as measured with the Quad GridPix detector using a generic drifter and a homogenous electric field. The gas mixture consist of 5% isobutane and 95% argon. Showing the detector's x y plane. Diffusion is clearly visible along with a distribution in arrival time shown by the colors (measured in time of arrival mode).

### 3.2. Strontium-90

The strontium-90 ( $^{90}\text{Sr}$ ) isotope decays by transforming a proton to a neutron or vice versa inside the nucleus. An electron is emitted. This decay is called beta<sup>-</sup> decay. In addition an antineutrino is created. The decay product is yttrium-90, which follows the same decay resulting in a stable state of zirconium. The net result is the emittance of electrons with an energy up to 2.28 MeV.

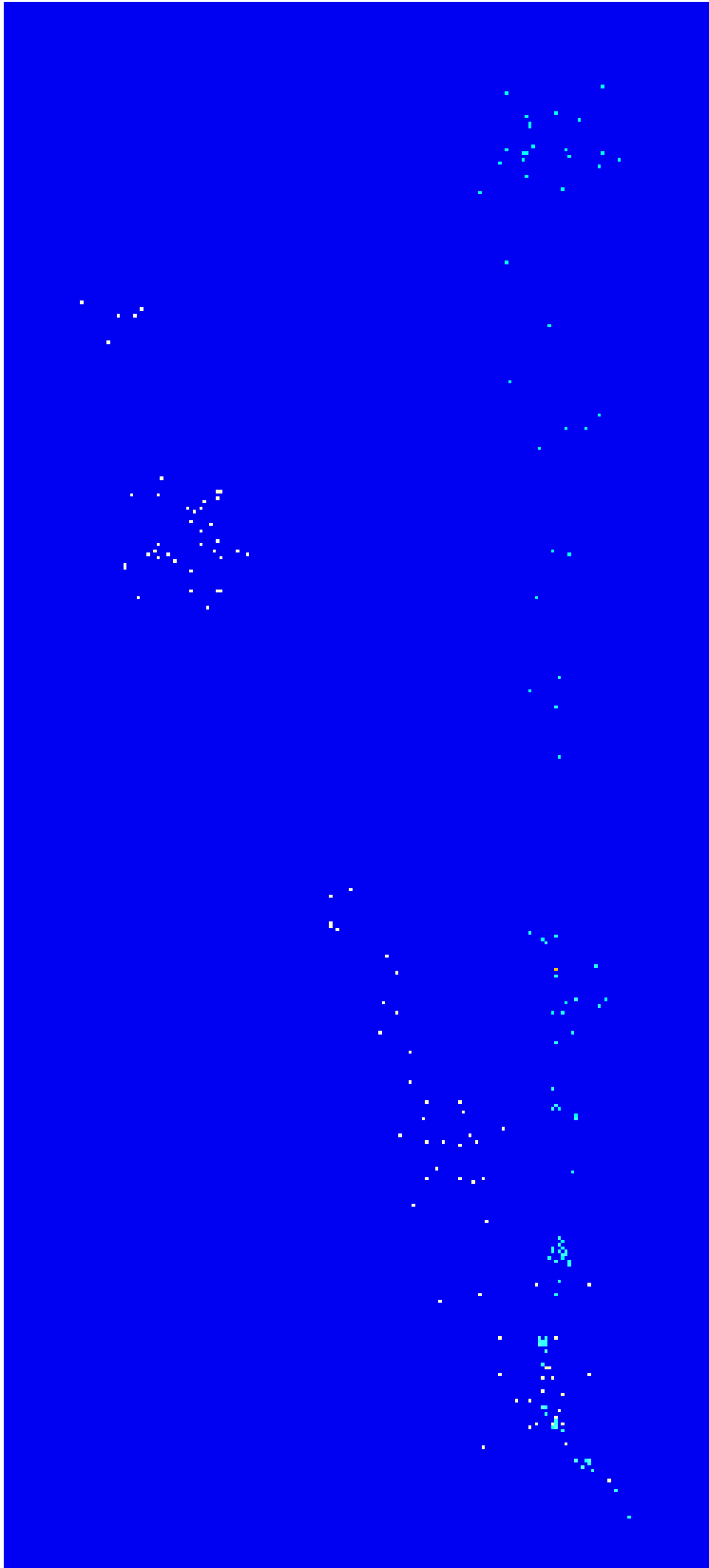


Figure 7. Two  $^{90}\text{Sr}$  tracks as measured with the Quad GridPix detector using a generic drifter and a homogenous electric field. The gas mixture consist of 5% isobutane and 95% argon. Showing the detector's x y plane. Both tracks cross two chips. The 'gap' in the tracks is due to the dead/non active inter chip regions. The color represent the arrival time (measured in time of arrival mode). The time difference in an individual track is minimal, indicating that the particle traversed the gaseous chamber parallel to the plane of the chips.

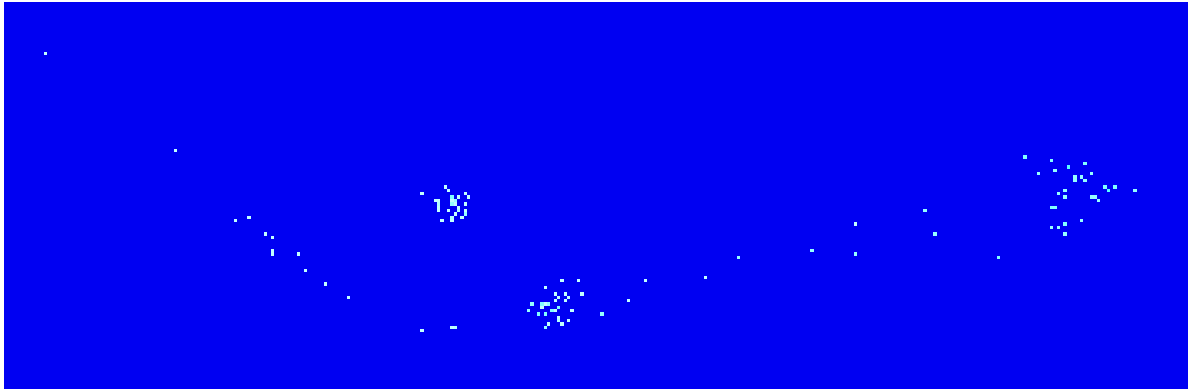


Figure 8. A  $^{90}\text{Sr}$  event as measured with the Quad GridPix detector using a generic drifter and a homogenous electric field. The gas mixture consist of 5% isobutane and 95% argon. Showing the detector's x y plane. Two tracks with the same origin are seen indicating that two electrons were ejected.

### 3.3. Alpha particles

The GridPix detector was used to measure alpha particles traversing the gaseous chamber. The source of those particles is an old gas mantle which contains thorium. Thorium has a decay chain involving many alpha decays. The thorium decay results in radon gas which can be flushed into the detector. The radon gas decays to polonium which decays further both through alpha decay. The later decay is relatively fast often resulting in two alpha particles with the same origin.

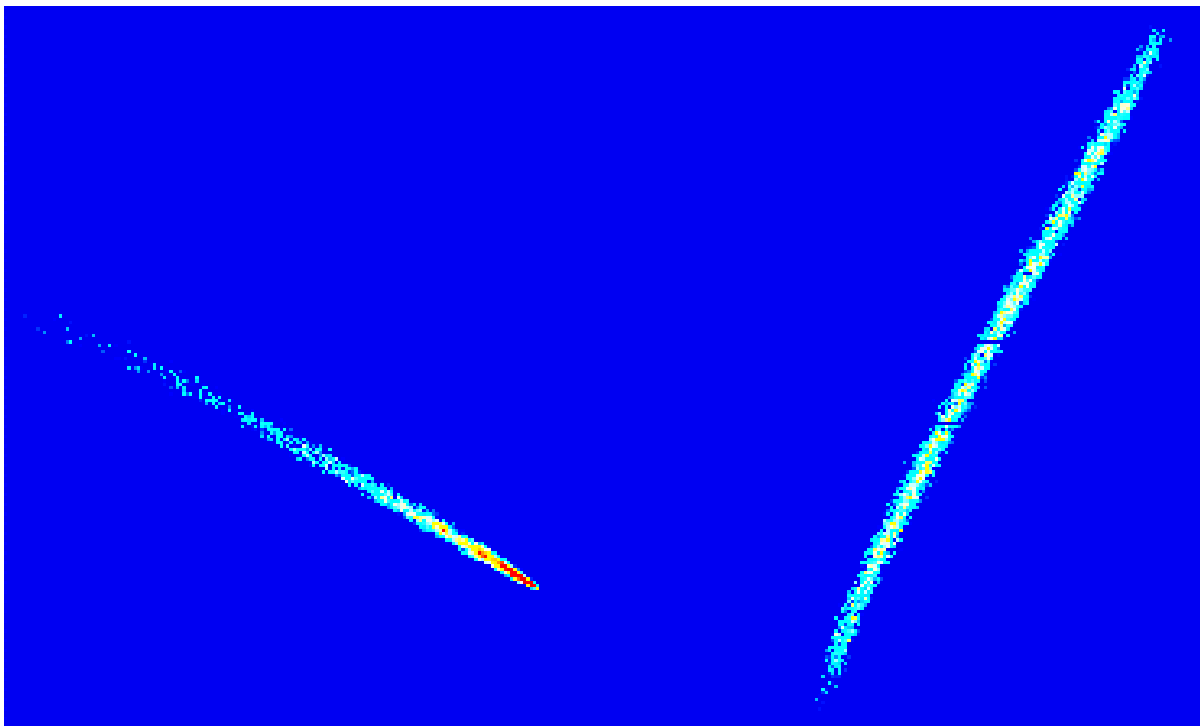


Figure 9. Two tracks of alpha particles as measured with the Quad GridPix detector using a generic drifter and a homogenous electric field. The gas mixture consist of 5% isobutane and 95% argon. Showing the detector's x y plane. The density of ionization is high as expected from a slow and heavy particle. The colors indicate the time (measured using time of arrival mode). Red indicates a short drift time (ionization close to the grid) in accordance with the lesser diffusion.

### 3.4. Cosmic rays and test beams

Cosmic particles are high energy radiation mostly originating from particles coming from outside the solar system. It produces showers of secondary particles that reach or penetrate the earth atmosphere or its surface. Products resulting from cosmic ray interaction with the atmosphere are called secondary cosmic rays. In general when referring to cosmic rays, muons are meant. Cosmic rays can be measured by placing the anode perpendicular to the earth's surface. The retrieved tracks are very straight, and in principle show virtually no variation in time.



Figure 10. A cosmic ray as measured with the Quad GridPix detector using a generic drifter and a homogenous electric field. The gas mixture consist of 5% isobutane and 95% argon. Showing the detector's x y plane. The color indicates the drift time which is equal for the whole track typical for cosmic rays (in principle, but depending on the test setup). Note the  $\delta$ -rays.

Test beams are experimental facilities at CERN (called Secondary Beams). A wide spectrum of particle beams are available. The various incident beams can supply protons, muons, electrons and others. Those particles traverse the experimental room in a straight line. Tracks retrieved are thus straight. Those facilitates also have magnetic fields present, allowing to conduct test under conditions with a magnetic field present.

## 4. Functioning of the Quad Focus GridPix Gaseous Tracking Detector

Four Timepix1-based GridPix chips were placed in a 2x2 configuration on a standard ReNext QUAD board. Each chip is wire bonded onto the PCB. Before placement of the chips, they were probed and classified. The correct readout was tested after placement of each individual additional chip. The high voltage supply of the grid for all four chips is common. This means that a discharge destroying one of the grids can potentially harm the other grids. As an additional measure of security, resistors were placed between each grid and the grid high voltage supply (100M  $\Omega$ ).

The Pixelman software was used to test for bad pixels by measurements of noise and the threshold adjustments were performed. This makes sure that the thresholds for each chip is mutually equal. The individual pixel threshold is adjusted with the 4 bits threshold adjustment. In addition, bad pixels were masked - those will not be actively read during data acquisitions. The software itself found 0.49% pixels not working correctly. Those are typically dead columns of which 5 were present. DAC scans were performed for each chip. The chip and software allow for a number of data acquisition settings. Not all are actively used but the chip's dependencies on those settings indicate whether or not the chip is functioning correctly. All four chips showed the same results according to the expected results of correctly functioning chips.

### 4.1. Preparation of the detector

The goal is to perform measurements and characterize the quad focus drifter by using the detector during test beams at CERN. Therefore the chips must perform correctly with high voltages supplied to the grid and the cathode and possibly large currents reaching the GridPix sensors (the protection layers need to function correctly). A generic drifter is applied on top of the ReNext QUAD board containing the 4 chips. The cathode foil has carbon applied on the inside. The drifter contains a field cage implemented with four copper strips. In between the cathode and the copper strips resistors of 4M7  $\Omega$  are placed. The resistor connecting the last strip to the ground is 1M  $\Omega$ . A schematic drawing of the drifter is shown in figure 11.

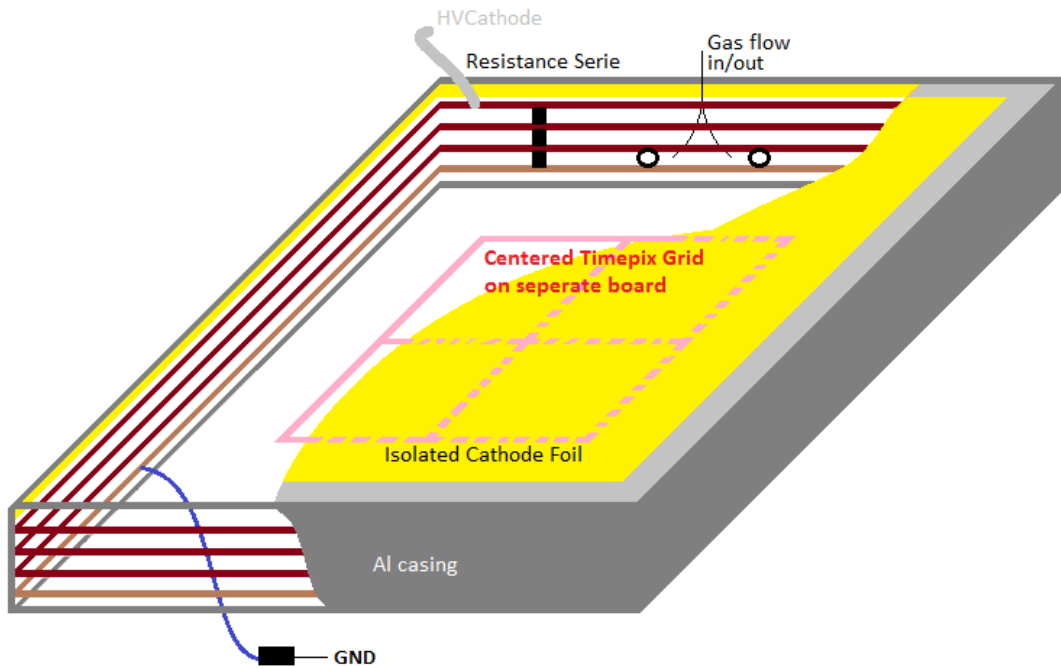


Figure 11. Schematic drawing of the test drifter.

The gas mixture used during those tests was isobutane (5%) and argon (95%). The whole detector is shown in figure 12 where guard is a name given to one of the high voltage power supply connections out of convention. In this implementation it connected to ground (the connection from the lowest copper strip to ground through a resistor). Normally a guard is an electrode above the grid with slight overlap to help shape the electric field and prevent strong fields at the end of the chips. For this setup an actual guard is not implemented.

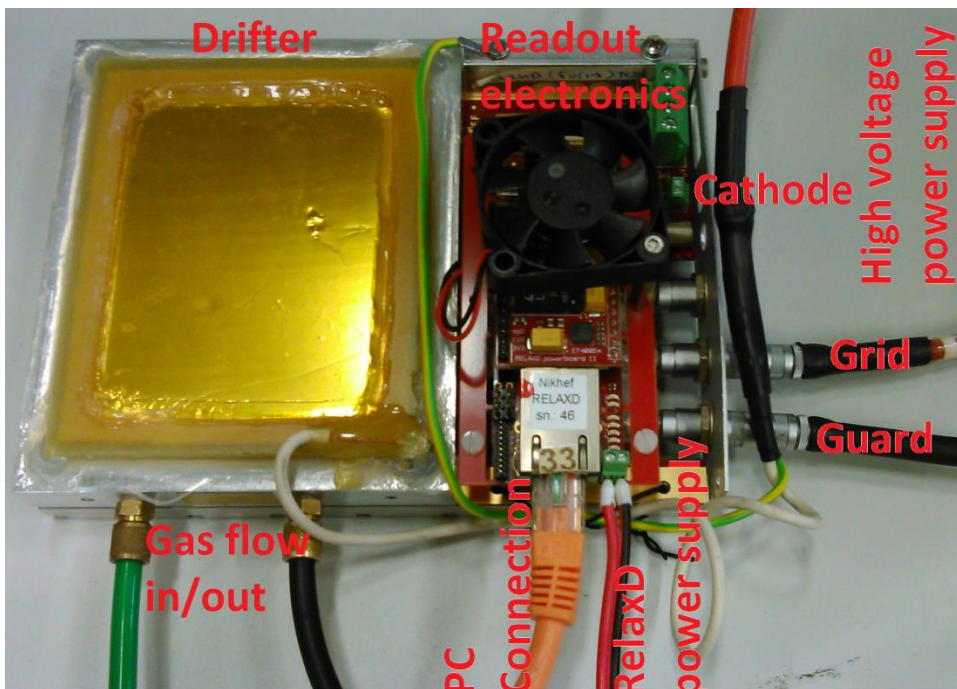


Figure 12. Setup of the connected detector with a generic drifter.

With -1000 V applied to the cathode and -320 V to the grid the setup shown in figure 12 was operated.  $^{55}\text{Fe}$  and  $^{90}\text{Sr}$  were held near the cathode and events were recorded (see chapter 3). The

orientation in which the matrix of chips is read was not corresponding to the actual orientation. With  $^{90}\text{Sr}$  the orientation has been assessed to be 3021, with 3 and 0 rotated up and 2 and 1 rotated down.

With a gas mixture of isobutane (5%) and argon (95%) and moderate high voltages (-1000 V applied to the cathode and -320 V to the grid), the detector showed good functionality by tracking various particles. The detector has acquired many frames of those events. The gas gains were moderate, but a discharging effect was visible were one or more chips would become over-activated – describable by a flash. This happens frequently. The wire bonds and the edges of the chips are not covered by glop-top. Furthermore this is a sign that indicates a high voltage breakdown of the chips but it is also an effect that can lessen or disappear over time. In fact it was observed that this effect seems to be lessened and the detector works stably at a grid voltage of -340 V, measuring Nikhef's  $^{55}\text{Fe}$  and  $^{90}\text{Sr}$  sources. During an early stage one chip might have broken down due to -360 V on the grid.

## 4.2. Cosmic ray measurements

As a longevity test, a setup is built to measure cosmic rays which will also be usable during the test beam. An aluminium rig containing the two scintillators, their photomultiplier tubes (PMT), used for the triggering mechanism, and the detector was made. The rig allows the detector to be mounted vertically horizontally. The detector is able to rotate approximately  $45^\circ$  in the plane of the anode to either side of its main orientation allowing for triggered measurements of straight tracks that can cover any two chips.

A trigger mechanism is made because timing of passing minimum ionizing particles is required for a correct measurement. Only when a cosmic ray traverses the detector's gaseous chamber a measurement should be made. The trigger logic is shown in figure 13. If the RelaxD module is not busy a trigger can occur. If a trigger occurs the shutter is opened during which the electrons are able to drift to the anode. After a trigger a second trigger is prevented by the RelaxD unit being busy and a 10 s veto timer.

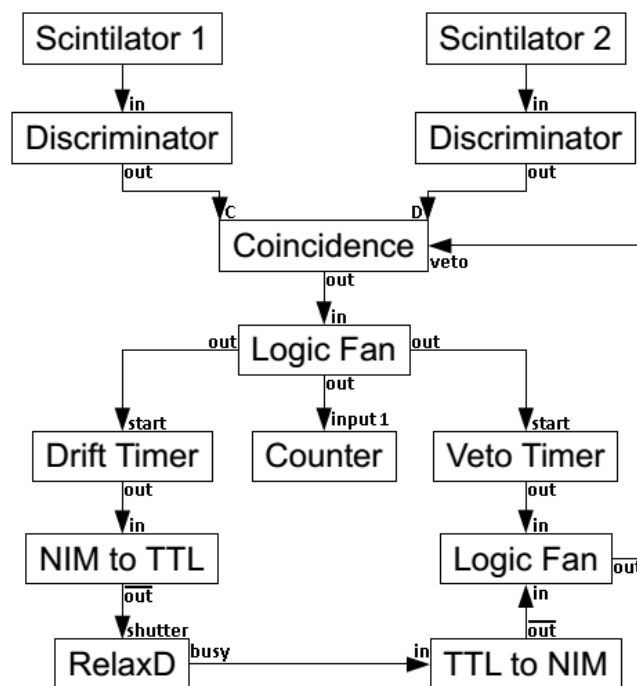


Figure 13. Trigger logic of the cosmic ray setup. The NIM/TTL converters are from POOL.

The detector ran for 1-3 days with a grid voltage of -340 V and cathode voltage of -1000 V. The measurements were conducted in Timepix mode (ToA). Figure 14 shows the raw plotted data of a measured cosmic ray. During those experiments two chips stopped functioning and needed to be replaced.

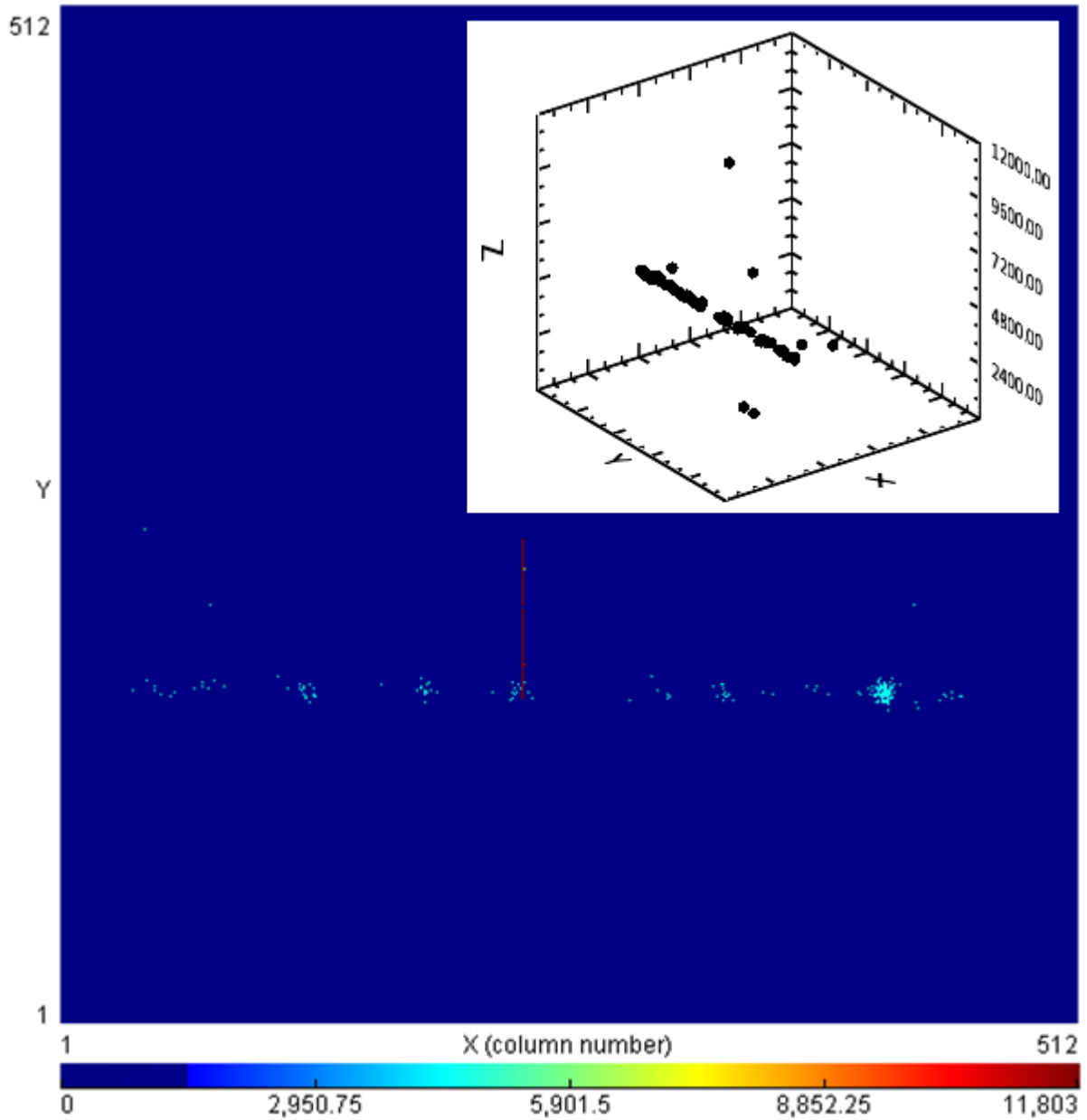


Figure 14. A cosmic ray track measured with the generic drifter. The XY plane displaying the 512x512 pixels. The Z axis displays an arbitrary time scale (raw data from a Time of Arrival measurement). The track is clearly visible, single scattered points can be due to bad pixels/noise.

# 5. The Quad Focus Drifter

In the development of the Quad Focus drifter itself many iterations have passed with varying success. The current existing drifter, the drifter that is being made for the calibration measurements and the current vision for a future quad focus drifter are discussed.

## 5.1. Initial design

An existing Quad Focus drifters is made of copper covered PCBs. Up to 16 PCBs are stacked on top of each other. With a 5 axis milling machine the inside is hollowed out to create the gaseous chamber. Figure 15 shows its design. The actual focusing part of the field cage consist of 8 PCBs. The other 8 (upper) create a homogenous electric field.

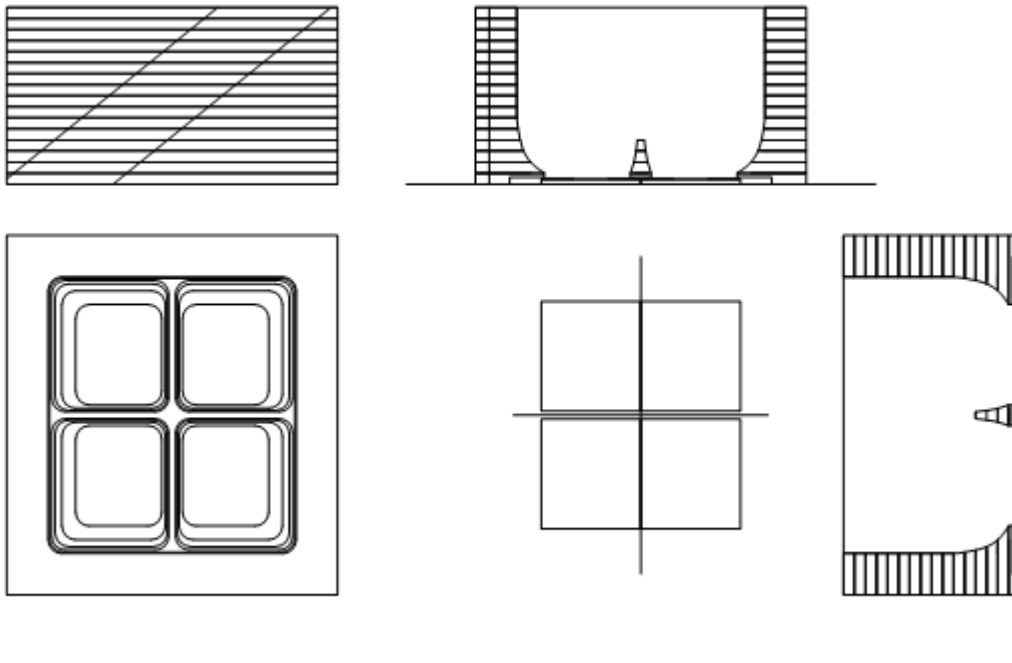


Figure 15. Schematic of the PCB Quad Focus drifter with the 2x2 chip matrix in the middle, the top view on the left and side views surrounding them.

## 5.2. Current design

The Quad Focus drifter will need to be measured using the nitrogen laser beam setup for calibration purposes. For this a new drifter is created consisting of the 8 lower PCBs, the half that focused, with on top of that a full glass window (BK7) of 20 mm high. This allows the laser beam with a maximum diameter of 15 mm and its focusing point of 6 mm to be focussed and translatable over the perpendicular electric field. The glass will have 8 copper strips or wirings that create the field cage. Furthermore the 8 PCBs are kept straight. Focusing of the electric field can be done by choosing the potentials of each field cage electrode. This allows for measurements with this drifter with both a focused and fully homogenous electric field for comparisons between the two. Its design is shown in figure 16. An O-ring is used to easily make a gas tight seal between the drifter and the ReNext QUAD board.

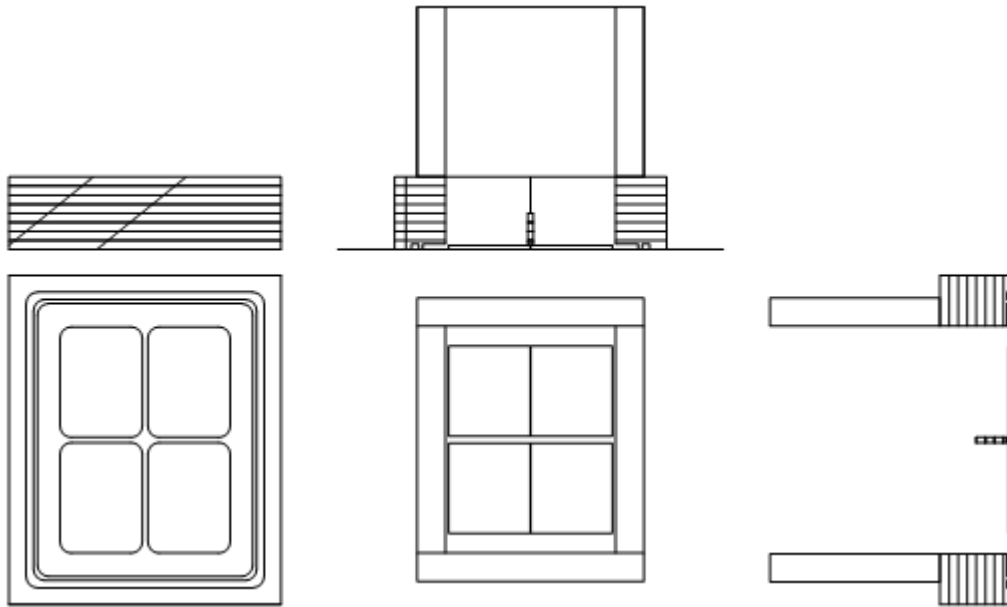


Figure 16. Schematic of the new Quad Focus drifter with the glass window. The 2x2 chip matrix and orientation of the window is shown in the middle, the top view on the left and side views surrounding them.

### 5.3. Outlook

Ultimately the drifter would be 3D printed with insulating and conducting materials that would have an intrinsic mechanism to allow connection to the high voltage supply for the field cage and cathode. The first attempt at a 3D printed Quad Focus drifter resulted in a structure that was not sufficiently gas tight. The material was too rough to be correctly bonded, over the chips, to the ReNext QUAD board. Improvements in 3D printing are constantly made and are promising for the realisation of the described design.

# 6. Tracking with the Quad Focus detector, its calibration and future measurements

The main purpose of the Quad Focus detector is to function with a non-homogenous electric field. This results in the requirement of new/extra calibration steps and verification of the whole principle. A nitrogen laser setup[5] will be used to measure the Quad Focus drifter with a homogenous field and focused field. The detector will be deployed in a test beam at CERN, here a magnetic field will be present and the retrieved tracks will be affected by this, however it is known that all those tracks are completely straight.

## 6.1. Simulations of the focused electric field

Before the first Quad Focus drifter was made, calculations were made of the electric field by using a finite element model that described the drifter (with incremented PCBs for the focusing half). Figure 17 shows those early results.

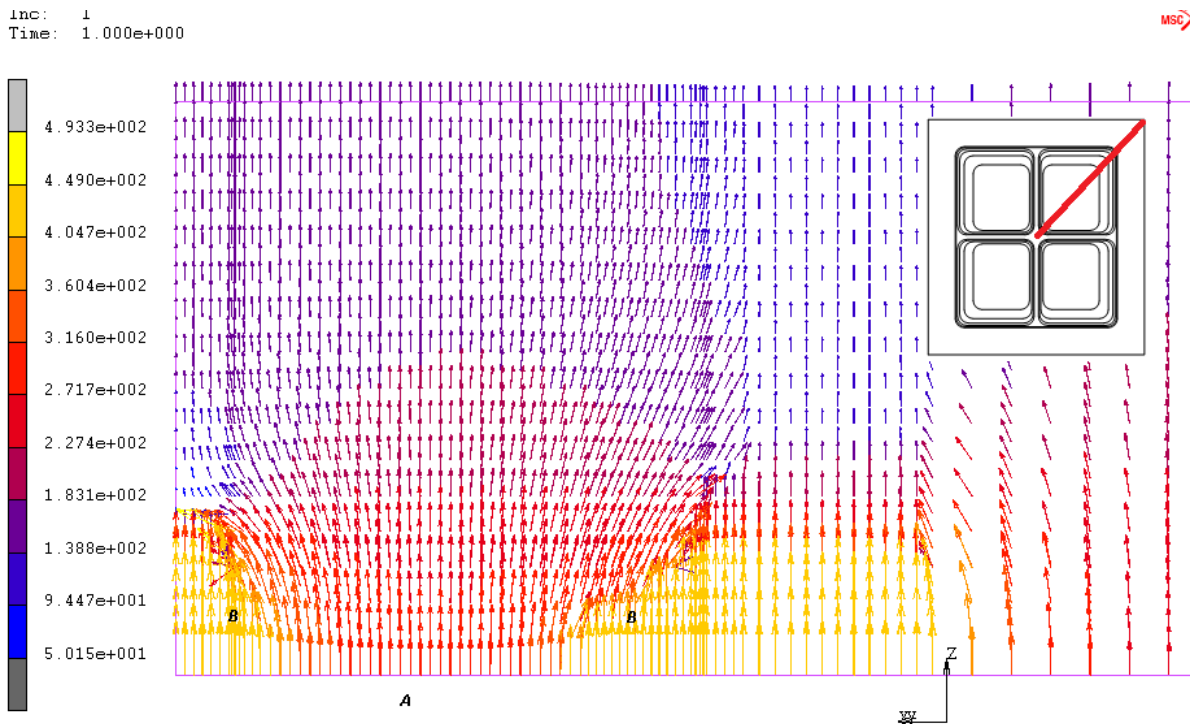


Figure 17. Calculation in three dimensions of the electric field for the first Quad Focus drifter based on a finite elements model. In the corner the orientation of this view is shown. The color indicates the intensity of the electric field and the arrow indicate the direction of the field. *A* indicates were the GridPix chips and thus the grid would be. *B* indicates the incremented PCBs.

If a strong correlation can be found between the electric field and the pixels hit by electrons from a known origin, the goal would be to form expressions that show a correlation between the origin

of an electron and the hit pixels while taking the electric field itself into account, such that the result could be used for other situations too.

## 6.2. Calibration of the Quad Focus drifter

The nitrogen laser can be used to create a very well defined ionization point in the conversion gap. A typical occupancy plot of hit pixels in a homogenous electric field with the strongest focusing of the laser is shown in figure 18a. The diffusion in the x direction (perpendicular to the laser beam) is small and depends on the electric field, the gas and z. Figure 18b shows the increasing width of the distribution of pixels hit with height.

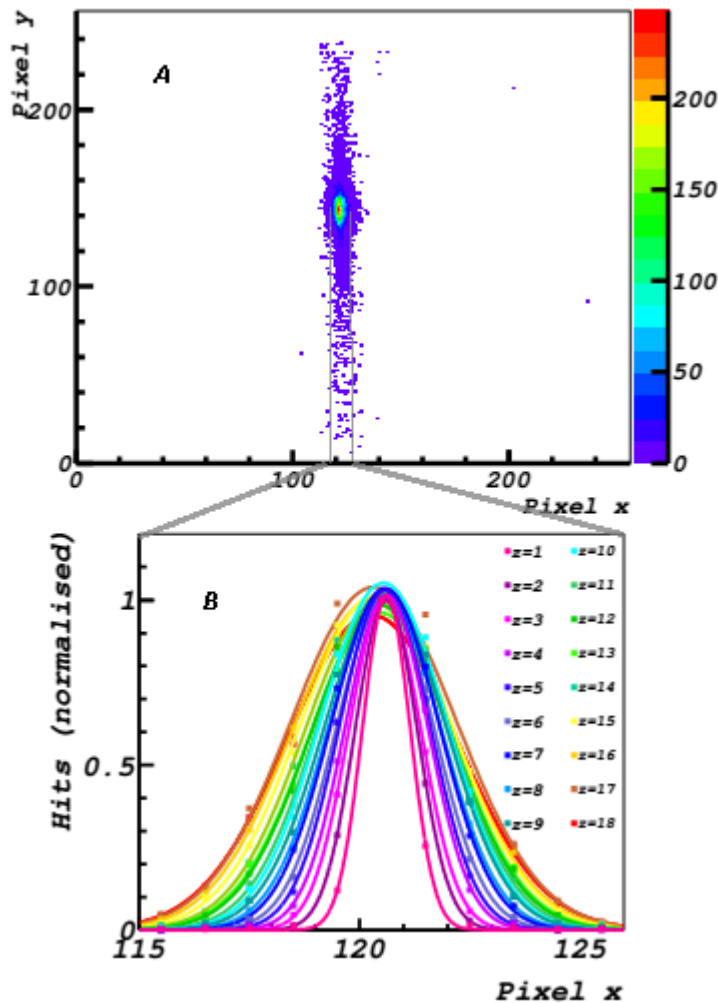


Figure 18. A) Occupancy plot of the hit pixels as a result from the lasers strongest focusing into the conversion gap of a GridPix detector with a homogenous field. B) Distribution of hit pixels as a function of height in a homogenous electric field.[4]

With the glass window drifter measurements can be conducted with the laser setup that replicate figure 18. The laser is translatable over the whole drifter. Scanning through the drifter with the laser focal point at  $f(x, y, z)$  a distribution of pixels hit is measured, resulting in a single hit pixel at  $f'(x', y')$ . Initially the conversion between  $f$  and  $f'$  will result in a look up table (matrix). The known focused electric field can act as the input for an initial look up table. The values of this matrix will be adjusted by using residuals retrieved from straight tracks fit to the test beam data. The effects of the magnetic field will be corrected for, which allows the original straight track to be reproduced.

# 7. Measurement of the specific resistivity of potential protection layers for GridPix

**A non-destructive in situ measurement of the specific resistivity of high resistive thin layers without a second contact electrode**

One component of the GridPix detectors is the protection layer on top of the pixels applied during wafer post processing. Such layers can be applied through various deposition techniques such as chemical vapour deposition and plasma enhanced chemical vapour deposition. The requirements of this layer for this specific application is a certain specific resistivity (ranging from  $10^7$  to  $10^{12}$   $\Omega\text{cm}$ ). This will protect against discharges to the readout chips caused by large currents while ensuring good functionality of the chip in general, i.e. no crosstalk – pixel input pads receiving substantial signal contribution from neighbouring pixel input pads.

In MEMS (Micro ElectroMechanical Systems) technology layers are made with a specific resistivity. For instance, insulating  $\text{Si}_x\text{N}_x$  can be made with high specific resistivity. During deposition a silane precursor and ammonia are merged together. By an excess of silane the layer becomes doped and silicon-rich nitride is formed, resulting in a lower specific resistivity. It is desirable to be able to measure the specific resistivity of those layers. This is typically done by applying a current perpendicular to the layer. Measuring the current magnitude and the voltage drop will allow to calculate a resistance value. To calculate the specific resistivity, it is necessary to have the current applied evenly over a certain known surface area. With prior art methods, involving various kinds of contact probes, it is difficult to measure the specific resistivity of thick and/or high resistive materials because a large contact area may be required. Resulting in that the actual contact size and the measured specific resistivity can be dependent on the contact pressure. Liquid contact electrodes, usually mercury, or the deposition of electrodes are used to overcome those problems. However this approach involves environmental hazards and/or the methods may be destructive to the specimen. Also some of those methods can affect the layer by creating junctions between the layer and electrode.

A new method is presented to overcome or reduce the above problems. A Micromegas is used to apply a homogenous shower of electron onto the layer. This allows for accurate measurements of the total current, surface area, and voltage drop, without contact and without destruction of the layer.

## 7.1. The Micromegas and measurement principles

The principals of this method stem from the Micromegas detector. The resistivity measurement uses a Micromegas structure as an electrode covering the layer. This is achieved by supporting a Micromegas foil with a frame which then can be placed on top of the layer. The foil is made of kapton with copper on either side. The foil is perforated with holes. One side contains photoresist insulating pillars. The non-pillar side is glued to the frame. The framed Micromegas is held on top of the resistive layer, shown in figure 19.

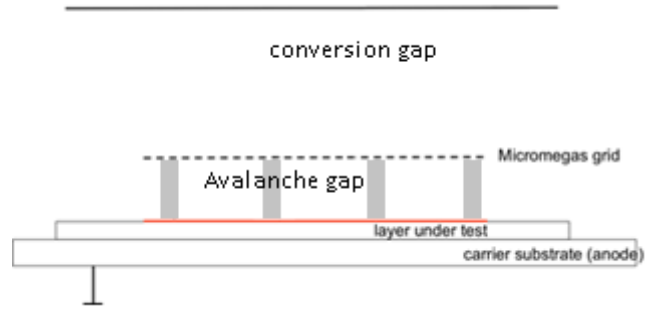
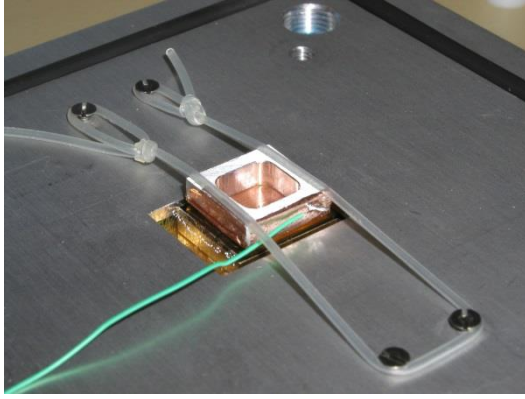


Figure 19. Left: an early setup showing a framed Micromegas on a resistive sample placed in an aluminum container. Right: a schematic drawing of the setup showing the resistive layer with a charge distribution in red. The pillars are shown, which keep the Micromegas grid at a defined distance.

Applying a high voltage to both the cathode and the Micromegas grid with the anode grounded introduces electric fields. The field in the avalanche gap is strong compared to the conversion gap. A single electron created in the conversion gap will pass through the grid, traversing the avalanche gap, resulting in an avalanche. This avalanche is able to deposit charge on a resistive layer. The strong electric field between the grid and the layer will cause any build up charge to be contained within the area where this strong electric field is applied, while the charge will still distribute itself evenly. Thus the charge creates an equipotential plane, the size of the fiducial area of the Micromegas. With the anode still at ground potential, any resistive layer can now be described by a capacitor and resistor parallel to each other.

## 7.2. The gas gain

A primary electron in the conversion gap causes an electron avalanche in the avalanche gap, this is the gas amplification process. It shows significant statistical fluctuations: the average gas gain however is well defined. The gas gain  $G$  increases exponentially with the potential over the avalanche gap, denoted here as the variable  $x$ .

$$G = A \exp(Bx) \quad 7.1$$

Were  $A$  and  $B$  are constants. For this method of main interest is the gas gain dependency on the grid voltage  $V_{grid}$ . The gas gain can double by an increase in  $V_{grid}$  with the gain doubling voltage  $V_D$ . Evaluating the gas gain results in

$$G = G_0 \exp\left(\frac{\ln 2}{V_D} V_{grid}\right) \quad 7.2$$

Were  $G_0$  equals 1 when equation 7.2 is used to describe the electron multiplication.

The above and following formulas omit potentials signs.

### 7.2.1. Measureable quantities

The gas gain supplies a constant homogenous DC current onto a resistive layer. The gas gain will reduce and stabilize due to a voltage drop over the resistive layer, now describable by a capacitor  $C$  and resistor  $R$  parallel to each other. The resistance can be calculated if the current  $I$  through the layer and the voltage drop  $V_T$  over the layer is known.

$$R = \frac{V_T}{I} \quad 7.3$$

The resistivity  $\rho$  can be calculated if the fiducial area of the Micromegas  $A$  and the layer thickness  $l$  is known.

$$\rho = \frac{V_T A}{I l} \quad 7.4$$

If there is a voltage drop  $V_T$  over the layer present the gas gain will be reduced as the electric field in the amplification gap is now reduced due to a reduced potential difference  $V_A$ .

$$V_A = V_{grid} - V_T \quad 7.5$$

Evaluating for the gas gain yields:

$$\begin{aligned} G &= G_0 \exp\left(\frac{\ln 2}{V_D} (V_{grid} - V_T)\right) \\ &= G'_0 \exp\left(-\frac{\ln 2}{V_D} V_T\right) \end{aligned} \quad 7.6$$

$V_T$  and  $I$  can be measured by supplying a gas gain. With a resistive layer present the gas gain will reduce until reaching a stable level. Shown in figure 20.

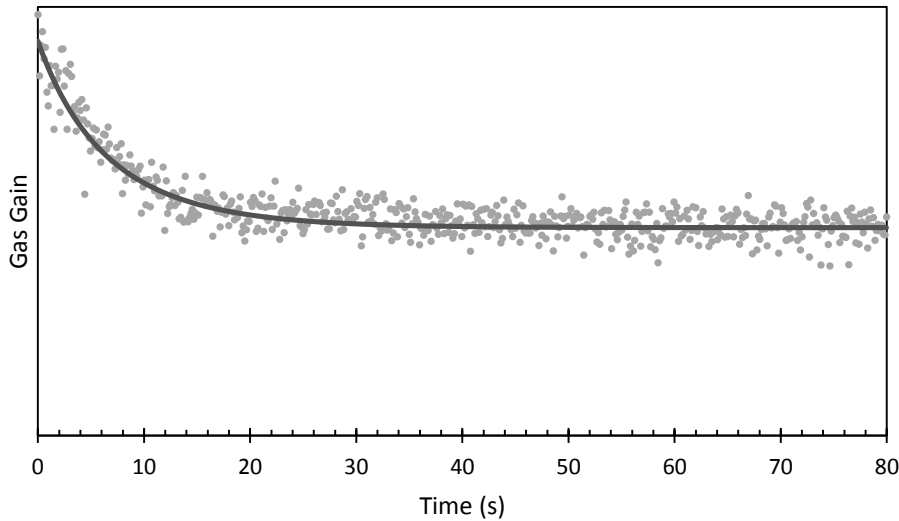


**Figure 20. Reduction of the gas gain over time to a stable state when a resistive layer is present. The**

$V_T$  can be calculated if the initial gas gain and the doubling voltage  $V_D$  is known. While measuring the current directly yields  $I$ . The doubling voltage can be accessed by measuring the gas gain as a function of  $V_{Grid}$  without a resistive layer present.

Evaluating the  $RC$  behaviour of the layer results in the time constant  $\tau$ .

$$RC = \rho \frac{l}{A} \epsilon_0 k \frac{A}{l} = \rho \epsilon_0 k = \tau \quad 7.7$$

Were  $\epsilon_0$  is the permittivity of vacuum and  $k$  the relative permittivity. If the layer has a voltage drop over it, allowing an IV measurement yielding  $R$  as described above the gas gain can be interrupted to allow the layer to discharge back to ground potential.

$$V_T(t) = V_{T,0} \exp\left(-\frac{t}{\tau}\right) \quad 7.8$$

The time constant  $\tau$  here is only dependent on the layers own characteristics. From equation 7.7 it follows that the time constant can be used to calculate the relative permittivity with the resistivity known or vice versa. The time constant can be measured through the gas gain. If the gas gain is terminated  $V_T$  follows equation 7.8. Substituting in equation 7.6 for the gas gain results in

$$G(t) = G_\infty \exp\left(-b \exp\left(-\frac{t}{\tau}\right)\right) \quad 7.9$$

With

$$G_\infty = G_0 \exp\left(\frac{\ln 2}{V_D} V_{grid}\right) \quad 7.10$$

$$b = \frac{\ln 2}{V_D} V_{T,0} \quad 7.11$$

Equation 7.9 describes the gas gain while the layer is discharging. In order to allow the layer to discharge no gas gain can be present. Equation 7.9 can still be measured by temporary introducing the gas gain at certain time intervals. Those measurements should be briefly enough to not contribute to recharging of the layer.

### 7.3. Experimental setup

A schematic drawing of the setup is shown in figure 21. Correct functioning of the setup during a measurement is validated using an oscilloscope, monitoring the pulses on the grid. Those pulses are due to ions drifting up. The same signal is measured by the LabVIEW data acquisition hardware. The current is measured from the resistive layer to the ground. The restive layer is put on a copper PCB which is connected to ground through an ammeter. The cathode, the Micromegas grid, the resistive layer and the PCB are sealed within a gas tight aluminium container.

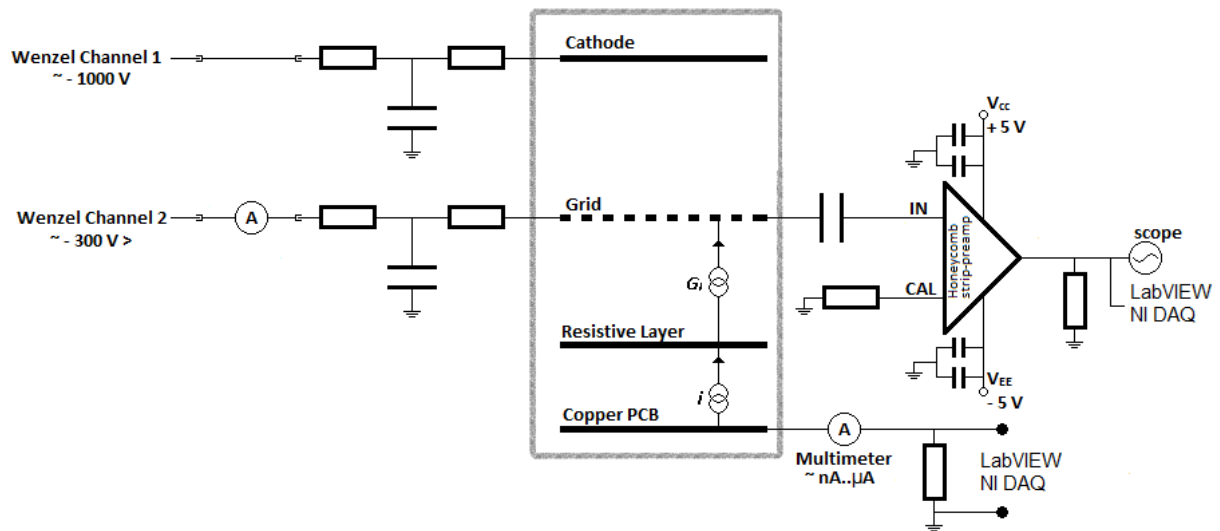


Figure 21. Schematic drawing of the resistivity measurement setup and its global electronic circuitry.

The setup is continuously flushed with a gas. Iron-55 is used as the ionization source. Electron-ion pairs are created in the conversion gap by ionization. The photo peak from the iron-55 spectrum can be used to quantify the gas gain. The reproducibility of this peak/spectrum depends on the quality of the Micromegas.

Between the framed Micromegas and the resistive layer, a thin Mylar foil is placed with a hole in it. It is used as a precaution for discharges at the edges of the framed Micromegas (the glue can make the foil uneven on the frame). The foil has a resistivity of  $10^{18} \Omega\text{cm}$ . If specimens with low resistivity relative to the Mylar foil are under test, the fiducial area  $A$  of the Micromegas is defined by this perforation as the electric field through the foil is several magnitudes smaller.

## 7.4. Results

Currently the limiting factor in the measurements is a Micromegas operating with a homogenous electric field. Appendix B shows various results of resistive layers while discharging. From those measurements the time constant was retrieved. However those measurements were performed during an early stage and the current was not measured, thus not showing the full potential of this method.

All samples measured are SiN samples supplied by either the Delft Institute of Microelectronics and Submicron Technology (DIMES), the Kavli Institute of Nanoscience Delft or Fraunhofer IZM, Berlin.

A reference measurement (equation 7.2) was performed on a gas mixture consisting of 95% argon and 5% isobutane, shown in figure 22.

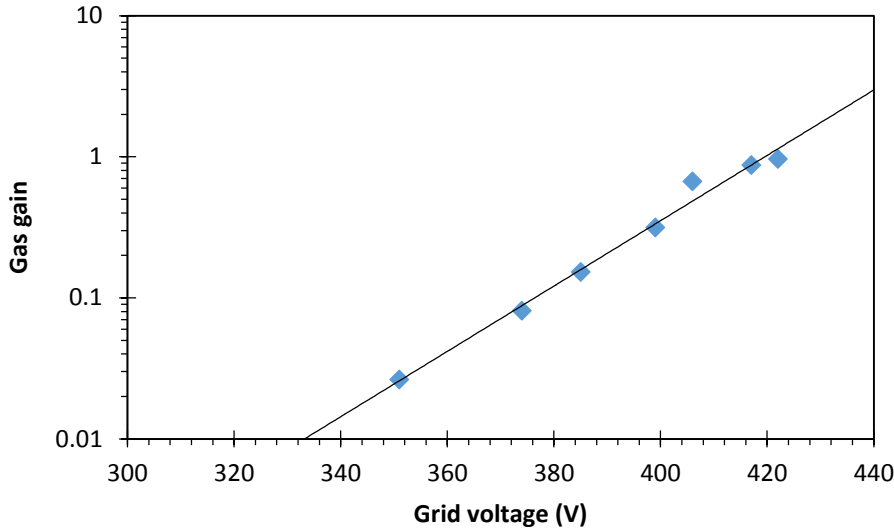


Figure 22. Reference measurement of the gas gain for a gas mixture consisting of 95% argon and 5% isobutane.

The measurement is fit to equation 7.2 resulting in

$$\frac{\ln 2}{V_D} = 0.053 \pm 0.003$$

The reported error is the standard deviation as resulted from the fit. Evaluating for  $V_D$  results in

$$V_D = 13.00 \pm 0.02 \text{ V}$$

This value is lower than the expected 18-21 V. This can be due to the Micromegas operating without a homogenous electric field. The measured gas gain values were accessed from the iron-55 spectrum. The measured spectrum did not result in a defined photo peak and did not allow for optimal recording of the gas gain.

A resistive layer was placed in the setup. A Mylar foil with a perforation with diameter 5 mm was placed between the Micromegas and the resistive layer. A gas gain was introduced with  $^{55}\text{Fe}$  and the layer was allowed to charge up. When the gas gain was reduced and stable the current through the resistive layer was measured by a picoammeter between the grid and power supply, resulting in 2.7 nA. The  $^{55}\text{Fe}$  source was removed and allowed to discharge back to ground potential, during which the gas gain was measured by short momentarily irradiations of the  $^{55}\text{Fe}$  source, resulting in figure 23.

**Table 1. The gas gain as a function of time during discharge of the resistive layer back to ground potential. Gas mixture 90% argon, 10% CO<sub>2</sub>. (Sample IZM gel pack H 7A.)**

$G$ $\pm 10$ (mV)	$t$ $\pm 5$ (s)
90	0
100	9.8
110	26.3
120	40.3
140	51.4
140	67.7
150	79.9
150	92.2
150	119.1
145	128.7
145	179.7

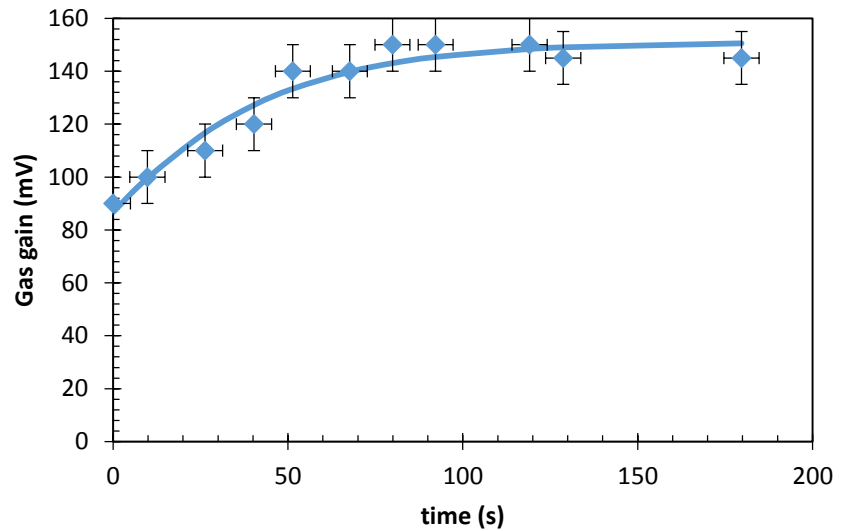


**Figure 23. The gas gain as a function of time during discharge of the resistive layer back to ground potential. Gas mixture 90% argon, 10% CO<sub>2</sub>. (Sample IZM gellpack H 7A.)**

The measurement was fit with equation 7.9 using gnuplot resulting in

$$\frac{\ln 2}{V_D} V_{t,0} = 0.55 \pm 0.05$$

$$\tau = 34 \pm 7 \text{ s}$$

From here the potential  $V_{t,0}$  on top of the resistive layer needs to be accessed. However  $V_D$  is required. The above measurements are not of the same gas mixture (the CO<sub>2</sub> gas mixture was used to serve as conveying the method as more appealing, concerning measurements reported in a paper. A reference measurement is not yet performed because the Micromegas did not work stably after this measurement was taken). However further calculations are made assuming  $V_D = 13.00 \pm 0.02 \text{ V}$ . This should be a good indication as argon is still the main component. This results in

$$V_{t,0} = 10.3 \pm 0.9 \text{ V}$$

The sample under test was measured to be 390 nm thick (ellipsometry performed by IZM). The measured current corresponds to  $V_{t,0}$ . The current (2.7 nA) is known and the fiducial area of the Micromegas is determined by the Mylar foil (a diameter of 5 mm). Calculating the resistivity  $\rho$  with equation 7.4 results in

$$\rho = (1.8 \pm 0.2) \cdot 10^{11} \Omega\text{m}$$

The resistivity of this sample was also measured by IZM, resulting in  $1.7 \cdot 10^{11} \Omega\text{m}$ . Confirming the measurement.

Furthermore, now that  $\rho$  and  $\tau$  are known,  $k$  can be calculated with equation 7.7 resulting in

$$k = 21 \pm 4$$

The resistive layer is a SiN thin film created by a plasma enhanced chemical vapour deposition process in which two precursors are merged together, namely ammonia and a silane precursor. Those two materials contribute to the eventual layer. The found  $k$  value is higher than expected but not higher than the value as reported for ammonia. With the thin film crystal structure, its purity and molecular composition unknown this value is very well possible. Most specifically  $k$  should be described as the static relative permittivity. It should be noted that the time constant was expected to be lower and judged to be in the lower range of measurable time constants. The time constant can possibly be lower if recharging of the layer did happen during the measurement, resulting in a slightly lower  $k$ .

## 7.5. Measurement remarks

Following the described measurement procedure it follows that very high resistivity's can be measured due to the dry gaseous environment and the strong electric field containing the charge within a defined area. High resistances are easier to measure because the time constant is large and recharging is virtually non-existent during the measurement. For a low resistivity the time constant also becomes lower, demanding a smaller time resolution for the measurements. Recharging will occur during the short irradiations. In practice, placing the  $^{55}\text{Fe}$  source at a greater distance from the conversion gap during discharge resulted in a much lower intensity of the gas gain, allowing for a continuous measurement of the gas gain while the layer was discharging. Low resistivity's of  $10^{10} \Omega\text{m}$  are measurable. The high resistivity limit is only dependent on the allocated measuring time. However, correctly fitting equation 7.9 to measurement data does not require a measurement as long as expected. The measurement time can potentially only last one  $\tau$ -time.  $G_{\infty}$  can be measured before charging the layer and can thus be eliminated as a fit parameter. Evaluating equation 7.9 for  $t = \tau$  shows that the percentile value were  $\tau$  occurs is dependent on  $V_T$ . Evaluation for  $t = 0$  shows that the initial value depends on  $V_T$ , it thus does not matter whether or not the resistive layer has been fully charged. The difference in the gas gain only has to be measurable. With  $G_{\infty}$  known, the measurement does not have to last till full depletion. However a longer measurement still is more accurate. Figure 24 shows equation 7.9 fit to measurement data, the data is fit with varying data points used. A measurement not lasting at least one  $\tau$ -time can potentially result in a lower  $\tau$ . The slope through  $t = 0$  is dependant on  $\tau$ . With fewer points this slope is more strongly influenced by the first data point resulting in a  $\tau$  with a larger error while it is less influential for the error in  $b$ . Appendix A helps in further understanding this function where the same principles have been used as a basis for a specific fit method for this function.

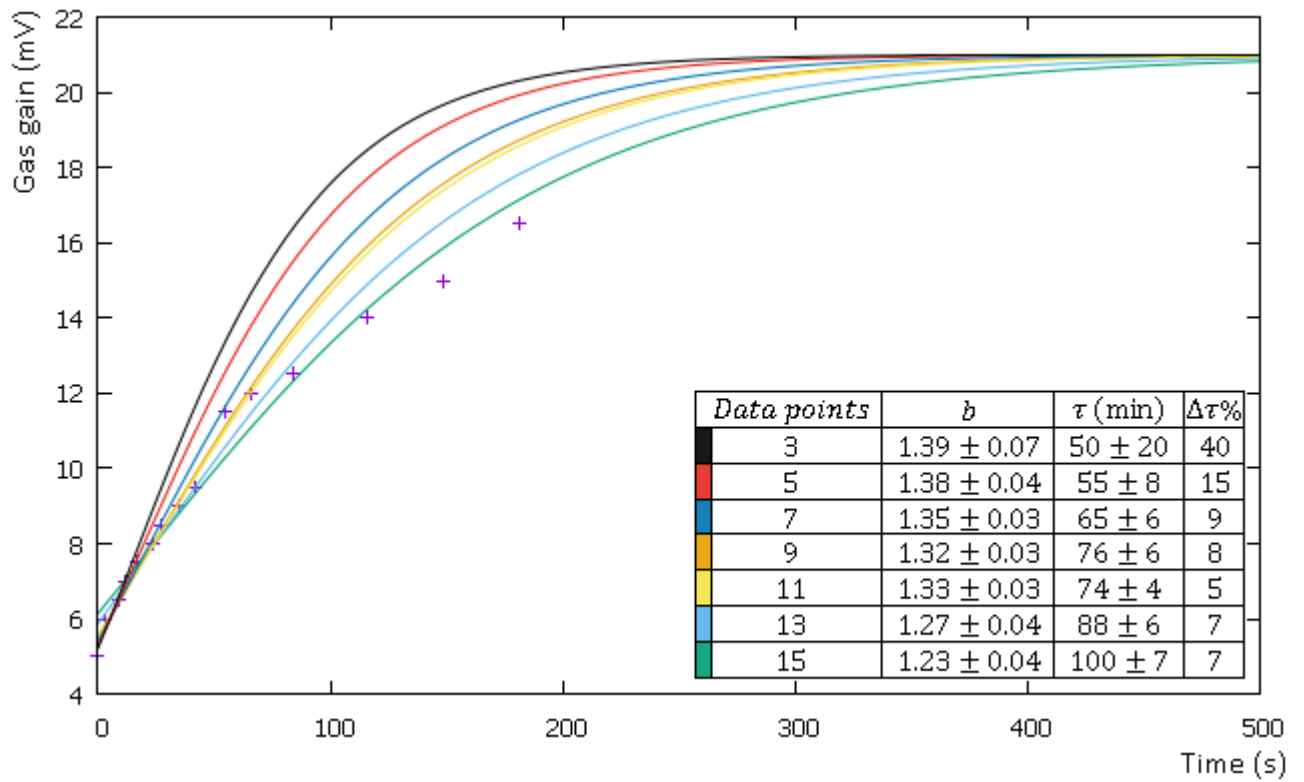


Figure 24. The gas gain as a function of time. Fit performed on a data series with gnuplot where  $G_{\infty}$  was kept constant (21 mV). A short measurement is possible but at the expense of precision in the retrieved values.

## 8. Conclusion

The development of the Quad Focus GridPix detector is well on its way. The current inevitable breakdown of the GridPix chips occurred, however before breakdown most chips showed correct functioning during operation. The broad outline of further steps that have to be taken in the development of the detector are very clear. The whole setup is nearing its completion, allowing for both calibration measurements using the nitrogen laser and track recording during a test beam in the near future.

A new method for the measurement of the specific resistivity involving a Micromegas is reported. The method allows for the measurement of virtually unlimited high resistivity. The strengths of this method, the possible ways in which to conduct a measurement and other suggestions for improvement are reported. The advantages stem from the dry gaseous environment and the strong electric field that is applied onto a resistive layer allowing for very precise measurements on a very large range, unlimited for high resistivity. The method is promising for applications in MEMS technology in general. The use of a Micromegas dismisses the need for a second contact electrode making in-situ measurements possible. A scientific paper will be published in a MEMS paper.

## 9. Future planning

The test setup for the Quad Focus drifter currently misses the new drifter. The new drifter is being made. The 8 stacked PCBs are nearing its completion. The glass window is actively being worked on. The existing high voltage supply will be tested with the old drifter in the near future. Once the high voltage supply is tested and functioning, the detector will be tested. The new drifter will be used for cosmic ray tests. If only the stacked PCB are finished, that portion will be temporarily covered with a copper cathode foil. This also provides a good opportunity to test the individual drifter components on being gas tight. The test will be conducted with a less diffusional gas mixture which requires stronger electric fields. This will be more representing of the conditions that will be used during the test beam measurements. When all parts of the drifter are finished it will be assembled into its final form. With the detector complete and functioning during cosmic ray measurements, test beam measurements can be conducted.

In summary

<b>(early)</b>	Glass window of drifter	PCB drifter	High voltage supply
<b>June</b>		Cosmic ray measurements with the detector	
<b>July</b>	Calibration measurements	Test beam measurements	

# Appendix

## A. A fit procedure for a Gompertz function

If measurement data is retrieved describing the gas gain as a function of time during discharging of the layer, the data needs to be fit. The expression follows the so called Gompertz function, with standard form

$$G = a \exp(-b \exp(-cx)) \quad \text{a.1}$$

$$a = G'_{\infty} \quad \text{a.2}$$

$$b = \frac{\ln 2}{V_D} V_{t,0} \quad \text{a.3}$$

$$c = \frac{1}{\tau} \quad \text{a.4}$$

$b$  and  $c$  are the main parameters to be defined in the fit. The procedure assumes that  $a$  is known, either through a separate measurement before the resistive layer was charged or as a value included in the measurement series, i.e.  $x \rightarrow \infty$ . The first step is the evaluation of this value through either of those methods. For the second step, finding  $b$ , the function is evaluated at  $x=0$  resulting in

$$G(0) = a \exp(-b) \quad \text{a.5}$$

Evaluating for  $b$  gives

$$b = -\ln\left(\frac{G(0)}{a}\right) \quad \text{a.6}$$

Assuming that a measurement value for  $G(0)$  exists,  $b$  can be calculated. Evaluating for  $G(1/c)$  results in

$$G\left(\frac{1}{c}\right) = a \exp\left(-\frac{b}{e}\right) \quad \text{a.7}$$

As both  $a$  and  $b$  are known the value for  $G(1/c)$  can be calculated. Searching for the closest corresponding value in the measured data will give an indication of  $c$ . Alternatively two measurement points covering the value of  $G(1/c)$  could be fit linearly for a more precise indication of  $\tau$ .

This method only uses a small percentage of the measured data points and thus the fit cannot be seen as the most reliable. Instead the proposed method takes the values obtained as initial values which can be iterated upon over a small range to find the best fit, i.e. by evaluating the  $R^2$  value. This iteration would take place for  $b$  and  $1/c$  and  $a$  if it was obtained from the measured data series  $G(x)$ . The iteration range would depend on the time interval of the measurement, especially for  $c$ .

## B. Resistive layer measurement results

### DIMES sample 3

This measurement was fit with both  $G'_\infty$  as a fit parameter and known.

$$G'_\infty = 28 \text{ mV}$$

Table 2. The gas gain (in mV) measured as a function of time (in seconds).

$G(t)$ (mV)	$t$ (s)
25	0
26.5	29
26.5	37
27	67
27	95
27.5	109
<b>28</b>	<b>600</b>

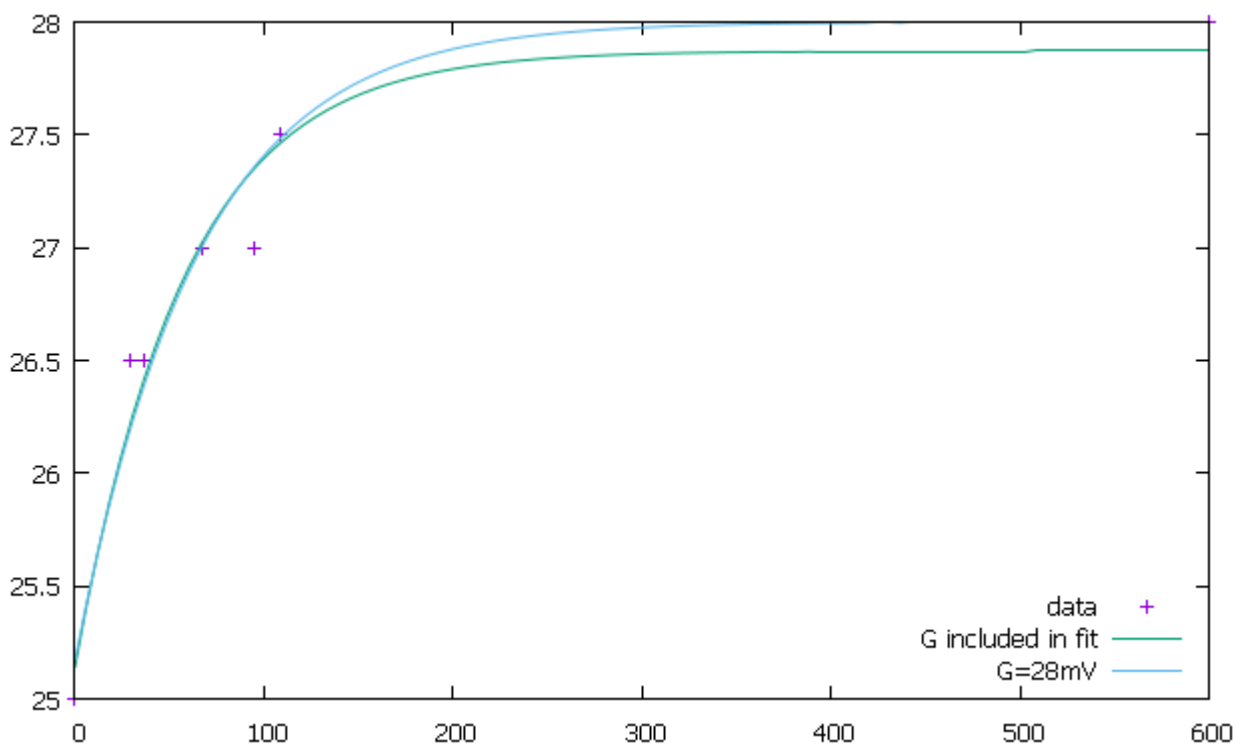


Figure 25. The gas gain (in mV) measured as a function of time (in seconds).

Table 3. Results for both fits.

Fit:	G included in fit	G=28mV
$\tau$ (s)	$55 \pm 13$	$62 \pm 8$

This measurement confirms that a full measurement is not needed but does improve the accuracy of the measurement as expected.

The spectroscopic ellipsometry measurements of figure 28 correspond to this sample.

# KAVLI 230 nm SiN

$$G'_\infty = 26 \text{ mV}$$

Table 4. The gas gain (in mV) measured as a function of time (in seconds).

$t$ (min)	$G(t)$ (mV)
0	14.5
8	15.5
38	17.5
53	18
77	18.5
92	20.5
105	20.5

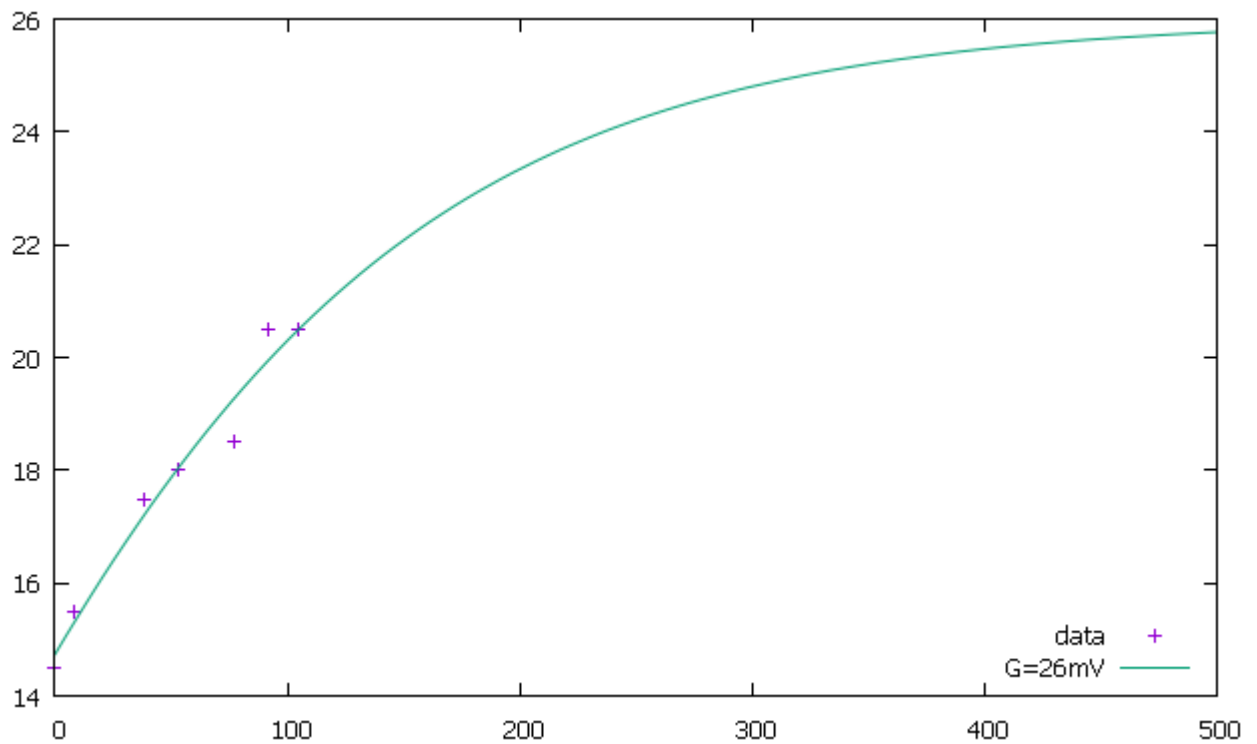


Figure 26. The gas gain (in mV) measured as a function of time (in minutes).

$$\tau \approx 2 \text{ hours}$$

## DIMES 662 nm SiN

$$G'_{\infty} = 21 \text{ mV}$$

Table 5. The gas gain (in mV) measured as a function of time (in seconds).

$t$ (min)	$G(t)$ (mV)
0	5
3	6
9	6.5
12	7
17	7.5
24	8
27	8.5
35	9
42	9.5
55	11.5
66	12
84	12.5
116	14
149	15
181	16.5

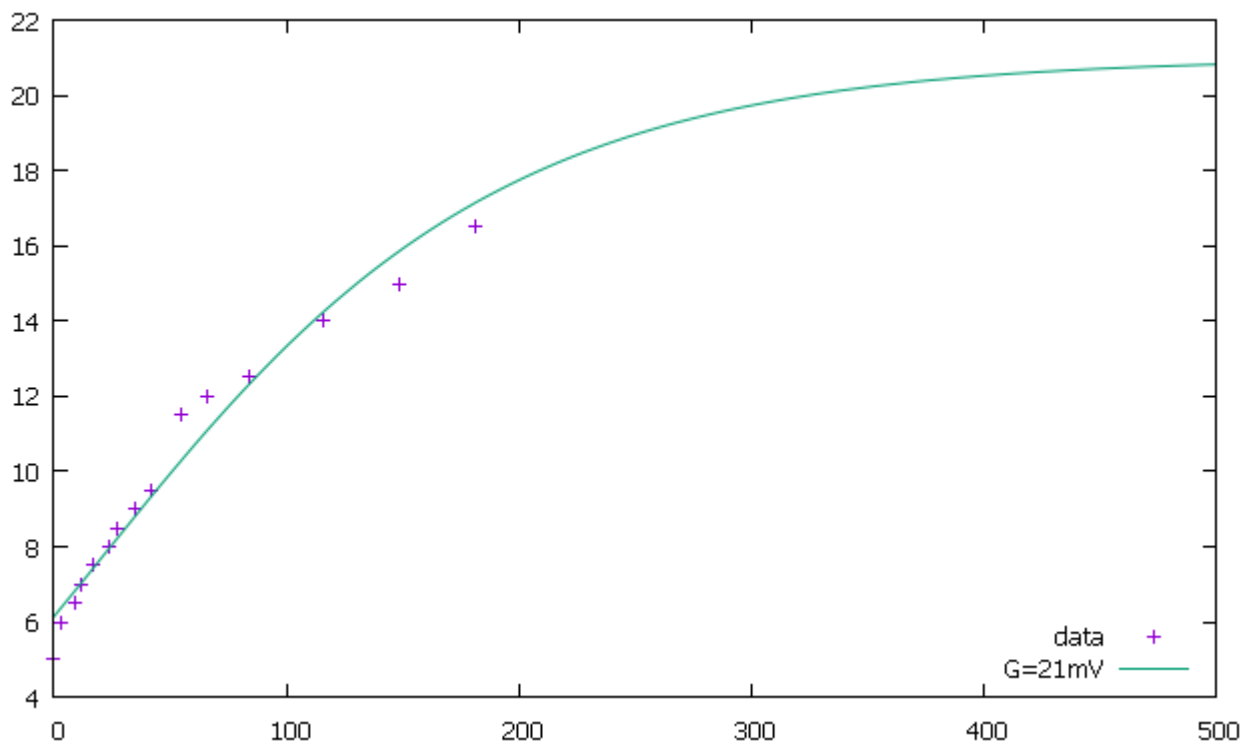


Figure 27. The gas gain (in mV) measured as a function of time (in minutes).

$$\tau \approx 1.5 \text{ hours}$$

This measurement was used in figure 23.

## C. Originele opdracht omschrijving

Project omschrijving Kevin van 't Veer

Stageperiode: 9feb 2015 –5 juni 2015

Dagelijks begeleider: Harry van der Graaf

Standplaats: Nikhef, Amsterdam

Grid Pix is een gas gevulde Time Projection Chamber met een uitlezing gebaseerd op de TimePix pixel chip, gecombineerd met een InGrid. In de ruimte tussen InGrid en de pixel chip treedt gas versterking op. Hiermee kunnen single electrons, achter gelaten door ioniserende straling, gedetecteerd worden in drie dimensies.

Een GridPix detector is in aanbouw die is voorzien van een speciale focusserende electrode. Hiermee wordt onderzocht in hoeverre het mogelijk is om de dode ruimte tussen twee pixel chips effectief te minimaliseren. Bij nog sterkere focussing is het wellicht mogelijk slechts een fractie van het uitlees oppervlakte bedekken met active pixels: dit leidt tot kosten besparing en een significante reductie van power dissipatie.

Kevin wordt betrokken bij de realisatie van deze test-detector, die uitgebreid zal worden getest op het Nikhef. Kevin zal vertrouwd worden gemaakt met de besturingsoftware van de TimePix pixel chips. De gehele opstelling zal worden getest door middel van een gefocuseerde UV laser beam, waarvoor een opstelling thans operationeel is op het Nikhef.

Zodra de detector goed functioneert zal deze getest worden in een deeltjes bundel op het CERN, Geneve. Het zal van de voortgang afhangen in hoeverre Kevin zich zal bezighouden met de analyse van de data die voortkomt uit deze test periode op CERN.

# References

- [1] FOM website, FOM institutes – Nikhef, February 2015
  
- [2] Nikhef website, departments – Detector Research & Development, February 2015
  
- [3] CERN Medipix website, February 2015
  
- [4] W.J.C Koppert, GridPix: Development and Characterisation of a Gaseous Tracking Detector – January 2015
  
- [5] F. Hartjes, A diffraction limited nitrogen laser for detector calibration in high energy physics – November 1990
  
- [6] S. van der Putten, GridPix: Measurements on a prototype micro time projection chamber – June 2006
  
- [7] Agilent, Basics of Measuring the Dielectric Properties of Materials Application Note – 2006

# Samenvatting

Een viervoudige Gridpix volg detector met een gefocuseerd elektrisch veld wordt gemaakt met als doel het uitvoeren van kalibratie en test metingen om de werking van de GridPix detectoren met een gefocuseerd elektrisch veld vast te stellen. Het totstand komen van de detector volgt een goed tempo. Zowel de kalibratie als test metingen zouden in de nabije toekomst mogelijk moeten zijn.

De detector is gebaseerd op de GridPix sensor, wat een Micromegas detector is gebaseerd op de Medipix chips. The Medipix chips zijn lading gevoelige CMOS chips op pixel basis. Specifiek wordt de TimePix1 gebruikt. Deze chips laten geklokte metingen toe, wat voor een extra meetbaar dimensie zorgt doormiddel van tijdmetingen. De Micromegas is een proportioneel detector en kan gezien worden als een twee dimensionale variatie van de Geiger teller.

Een kathode folie wordt boven een gaas structuur of rooster geplaatst, welke met isolerende pilaren op de uitlees anode rust. Er staat een hoge spanning op de kathode en het gaas, wat elektrische velden creëert. Het elektrisch veld tussen het gaas en het uitlees mechanisme is vele malen groter dan het veld boven het gaas. Het geheel is gevuld met een gas. Een geladen energetisch deeltje kan het gasvolume passeren; dit ioniseert het gas. Een elektron of clusters van elektronen worden vrijgemaakt. De elektronen volgen het elektrisch veld richting de anode. Wanneer zij het rooster passeren worden **ze** versneld wat er voor zorgt dat een elektron een tweede elektron kan vrijmaken welke ook weer een tweede elektron kan vrijmaken. Een elektronen lawine wordt gecreëerd, groot genoeg om gedetecteerd te worden. In het geval van de GridPix sensor is het uitlezen gebaseerd op de Medipix chips. Het rooster is opgenomen op de GridPix chip zelf. Elk gat in het rooster komt overeen met een pixel. Dit wordt gerealiseerd door wafer nabewerking.

In het verleden zijn de GridPix gasgevulde detectoren getest met een homogeen elektrisch veld. De huidige detector zal een gefocuseerd elektrisch veld gebruiken, wat de productie kosten kunnen verbeteren. Er is een kleiner uitlees oppervlakte nodig is om het zelfde of een groter gas volume uit te lezen. Hiervoor zijn kalibratie metingen nodig om voor het niet homogeen elektrisch veld te corrigeren. Bij metingen met een test straal zal een magnetisch veld aanwezig zijn. Dit zal effect hebben op de metingen omdat het elektrisch en magnetisch veld niet volledig parrallel aan elkaar staan. De mogelijkheden voor het consistent toepassen van de correcties, benodigd wanneer een magnetisch veld meespeeld, zal vast gelegd worden.

De gasgevulde volg detectoren zijn veel belovend als volg detectoren voor toepassingen in bijvoorbeeld het ATLAS experiment. Deze detectoren kunnen een deel van een spoor waarnemen op basis waarvan het gehele spoor achterhaald kan worden. Op dit moment worden alleen op halgeleider materiaal gebaseerde detectoren gebruikt. Die geven alleen een twee dimensionaal punt waarmee een totaal spoor moet worden achterhaald.

Een onderdeel van de GridPix detectoren is de beschermingslaag boven op de pixels. Onderzoek naar het verbeteren van die laag heeft geresulteerd in het ontwikkelen van een nieuwe methode om de (hoge) specifieke weerstanden van dunne films te meten. Deze methode is gebaseerd op de Micromegas detector.

# Dankwoord

Graag zou ik alle studenten en andere betrokkene willen bedanken die nu werken of in het verleden hebben gewerkt projecten van detector R&D. Bij elkaar hebben zij veel literatuur achtergelaten. Graag zou ik Joop willen bedanken voor al zijn ondersteunende werkzaamheden. Dat geldt ook voor Wim, Oscar, René en Eric. The students and others over at Delft, DIMES, KAVLI and IZM for the SiN's and their assistance were needed for the resistivity's. Ook wil ik Fred bedanken voor zijn inspiratieve inzichten en hulp. Natuurlijk wil ik ook Harry van der Graaf bedanken voor deze stage in het algemeen en voor het zijn van de meest enthousiaste begeleider die ik me kan voorstellen.